Synthesis, Photophysical Properties, and Photovoltaic Devices of Oligo(*p*-phenylene vinylene)-fullerene Dyads[||]

Emiel Peeters,[†] Paul A. van Hal,[†] Joop Knol,[‡] Christoph J. Brabec,[§] N. Serdar Sariciftci,[§] J. C. Hummelen,[‡] and René A. J. Janssen*,[†]

Laboratory of Macromolecular and Organic Chemistry, Eindhoven University of Technology, P.O. Box 513, 5600 MB Eindhoven, The Netherlands, Stratingh Institute and MSC, University of Groningen, Nijenborgh 4, 9747 AG Groningen, The Netherlands, and Christian Doppler Laboratory for Plastic Solar Cells, Johannes Kepler University Linz, Altenbergerstrasse 69, A-4040 Linz, Austria

Received: May 8, 2000; In Final Form: August 31, 2000

The synthesis of a homologous series of oligo(*p*-phenylene vinylene)-fulleropyrrolidines (OPV*n*-C_{60}, $n = 1-4$, where n is the number of phenyl rings) is described. The photophysical properties of these donor−acceptor dyads and the corresponding model compounds, α,ω-dimethyl-2,5-bis(2-(*S*)-methylbutoxy)-1,4-phenylene vinylene oligomers (OPV*n*, $n = 2-4$) and *N*-methylfulleropyrrolidine (MP-C_{60}), are studied as a function of the conjugation length in solvents of different polarity and as thin films. Fast singlet energy transfer occurs after photoexcitation of the OPV*n* moiety of the dyads toward the fullerene moiety in an apolar solvent. Photoexcitation of the dyads in a polar solvent results in electron transfer for OPV3-C_{60} and OPV4-C_{60}, and to some extent for OPV2-C_{60}, but not for OPV1-C_{60}. These results are compared to the results obtained for mixtures of OPV*n* and MP-C_{60} in the same solvents. The solvent-dependent change in free energy for charge separation of the donor−acceptor systems is calculated from the Weller equation, and the rate constants for energy and electron transfer are derived from the fluorescence lifetime and quenching. The results show that in a polar solvent electron transfer in these dyads is likely to occur via a two-step process, that is, a very fast singlet energy transfer prior to charge separation. In thin solid films of OPV3-C_{60} and OPV4-C_{60}, a long-lived charge-separated state is formed after photoexcitation. The long lifetime in the film is attributed to the migration of charges to different molecules. A flexible photovoltaic device is prepared from OPV4-C_{60}.

Introduction

Photoinduced charge transfer between π-conjugated polymers and fullerene C_{60} is of considerable interest for photovoltaic energy conversion using organic and polymer materials as an active layer. Time-resolved spectroscopy has revealed that photoinduced electron transfer in polymer−fullerene blends occurs in the femtosecond time domain, several orders of magnitude faster than the radiative or other nonradiative decay processes.[1−3] Therefore, the quantum efficiency of photoinduced charge separation across the donor−acceptor (D−A) interface in these mixtures is assumed to be close to unity. The efficient charge separation in these mixtures is assisted by the large interfacial area between donor and acceptor phases, which is formed spontaneously during spin coating.[4] Surprisingly, the back electron transfer is orders of magnitude slower than the photoinduced forward electron transfer and the charge-separated state persists even in the microsecond and millisecond time domains.[1,5] The large asymmetry between forward and backward electron-transfer rates in these bulk heterojunctions enables the collection of photoinduced charges.[6,7] At present, the energy conversion efficiency of these photovoltaic cells is restricted by the carrier collection efficiency and the limited charge carrier mobility in disordered homogeneous blends. Therefore, studying photovoltaic efficiency in relation to morphology and mesoscopic ordering in the active layer is of profound interest.[8]

The rapid advancement in fullerene chemistry allows the covalent functionalization of C_{60} with electron donors.[9] In recent years, many C_{60}-based donor−acceptor dyads have been synthesized and investigated to gain insight into the intramolecular photophysical processes, such as energy and electron transfer.[10] Although these dyads can serve as model compounds for the π-conjugated polymer−fullerene photovoltaic cells, only a few examples have been reported in which π-conjugated oligomers are covalently attached to C_{60}.[11−15] Apart from being well-defined model systems for photophysical characterization, the covalent linkage between donor and acceptor in these molecular dyads provides a simple method to achieve dimensional control over the phase separation in D−A networks.

Here, we report the synthesis of a homologous series of well-defined donor−C_{60} dyad molecules with a π-conjugated oligo(*p*-phenylene vinylene) as the donor moiety (OPV*n*-C_{60}, $n = 1-4$, where n is the number of phenyl rings; see Figure 1).[16] We have studied the photophysical properties of these oligo(*p*-phenylene vinylene)-fulleropyrrolidines in detail, both as single molecules in solution and as assemblies in thin films, and the results are compared to those of mixtures of *N*-methylfulleropyrrolidine (MP-C_{60}) and a series of α,ω-dimethyl-

* Corresponding author. Phone: (+)31.40.2473597. Fax: (+)31.40.2451036. E-mail: r.a.j.janssen@tue.nl.

[||] Dedicated to Professor Fred Wudl on the occasion of his 60th birthday in acknowledgment of his seminal contributions to the chemistry and physics of conjugated polymers and fullerenes.

[†] Eindhoven University of Technology.
[‡] University of Groningen.
[§] Johannes Kepler University Linz.

10.1021/jp001717b CCC: $19.00
Published on Web 10/19/2000

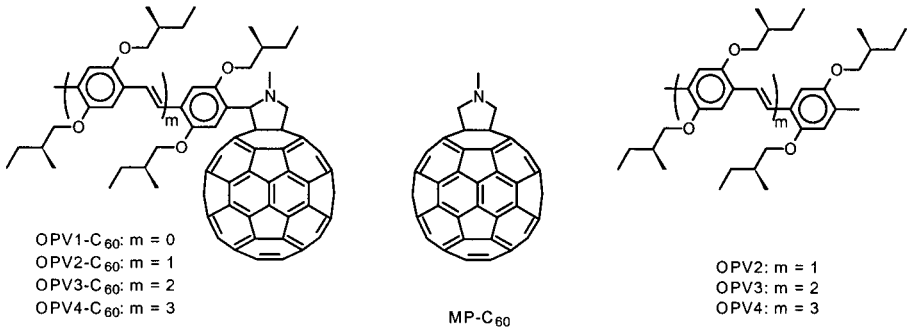

Figure 1. Structure of OPV*n*-C_{60} dyads and OPV*n* and MP-C_{60} model compounds.

SCHEME 1

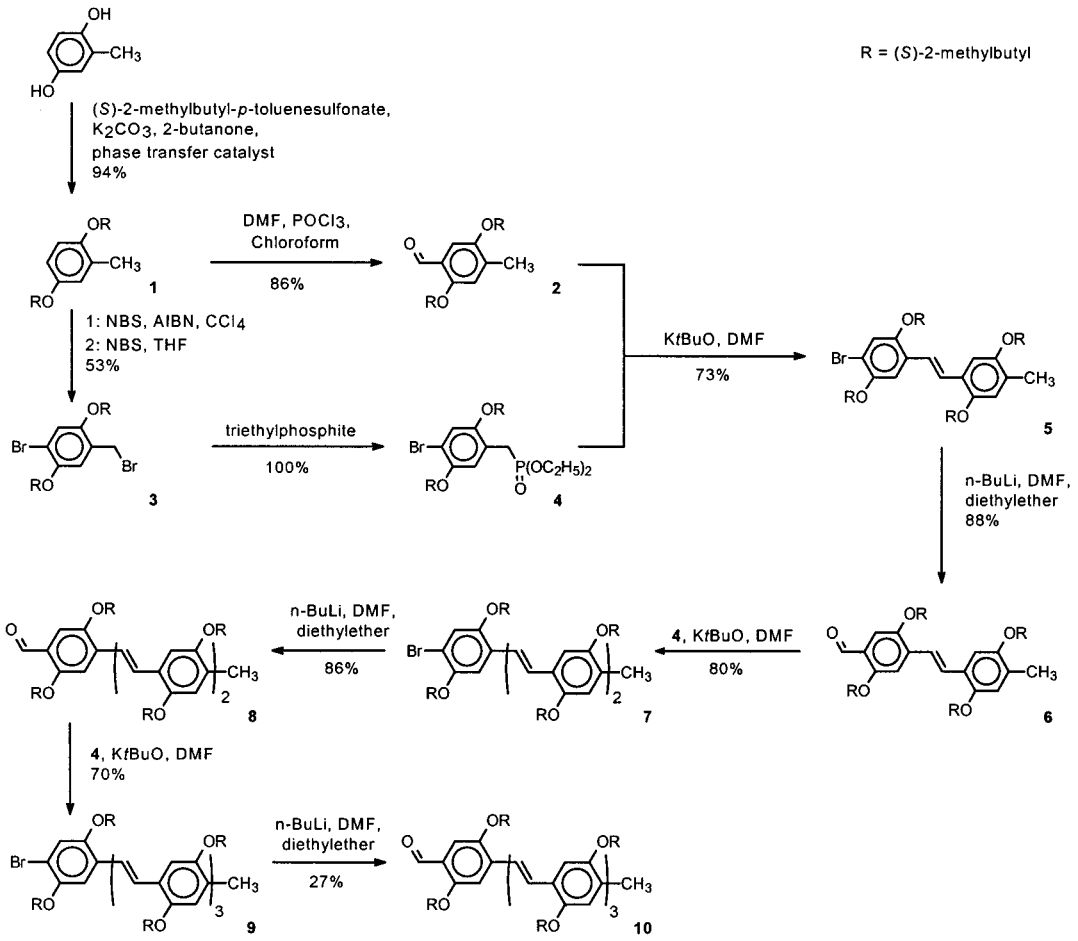

oligo(*p*-phenylene vinylene)s (OPV*n*'s, $n = 2-4$; see Figure 1). We demonstrate that both energy and electron transfer occur in solution on short time scales. The differentiation between the two processes depends on the conjugation length of the oligomer and the polarity of the solvent. In apolar solvents, we invariably observe energy transfer, whereas in more polar solvents photoinduced electron transfer occurs for $n = 3$ and 4 and to some extent for $n = 2$. From fluorescence spectroscopy, we infer that the electron transfer in polar solvents is likely to be preceded by energy transfer and, hence, occurs in a two-step process. The discrimination between energy and electron transfer is semiquantitatively accounted for by the Weller equation for photoinduced charge separation.[17] In thin solid films, we observe photoinduced electron transfer for the two longest systems, that is, OPV3-C_{60} and OPV4-C_{60}. Using the latter as the single photoactive material, a working photovoltaic cell has been demonstrated.

Results and Discussion

Synthesis. The oligo(*p*-phenylene vinylene)s, **6**, **8**, and **10**, containing an aldehyde functionality, were synthesized by applying the Wittig−Horner coupling reaction (Scheme 1).[18] A Williamson etherification of methylhydroquinone with enantiomerically pure (*S*)-2-methylbutyl-*p*-toluenesulfonate gave 1,4-bis[(*S*)-2-methylbutoxy]-2-methylbenzene, **1**, in 94% yield. Subsequent formylation of **1** using phosphorus oxychloride and *N*,*N*-dimethylformamide (DMF) in refluxing chloroform gave aldehyde **2** in 86% yield after column chromatography and recrystallization. Compound **3** was isolated in 53% yield by radical bromination of **1** with 1.2 equiv of *N*-bromosuccinimide (NBS) and 2,2′-azobis(2-methylpropionitrile) (AIBN) in dry refluxing carbon tetrachloride followed by ionic bromination of the intermediate with 1.3 equiv of NBS in dry refluxing tetrahydrofuran. Phosphonate **4** was obtained from **3** by a

SCHEME 2

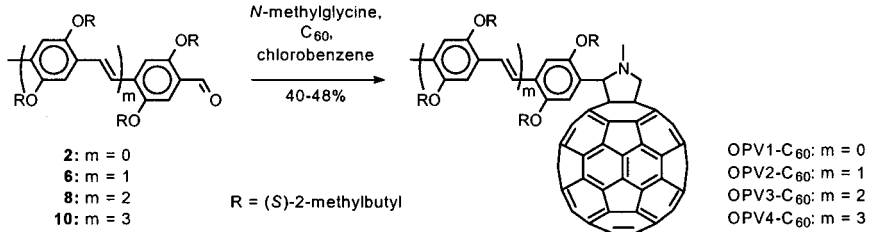

SCHEME 3

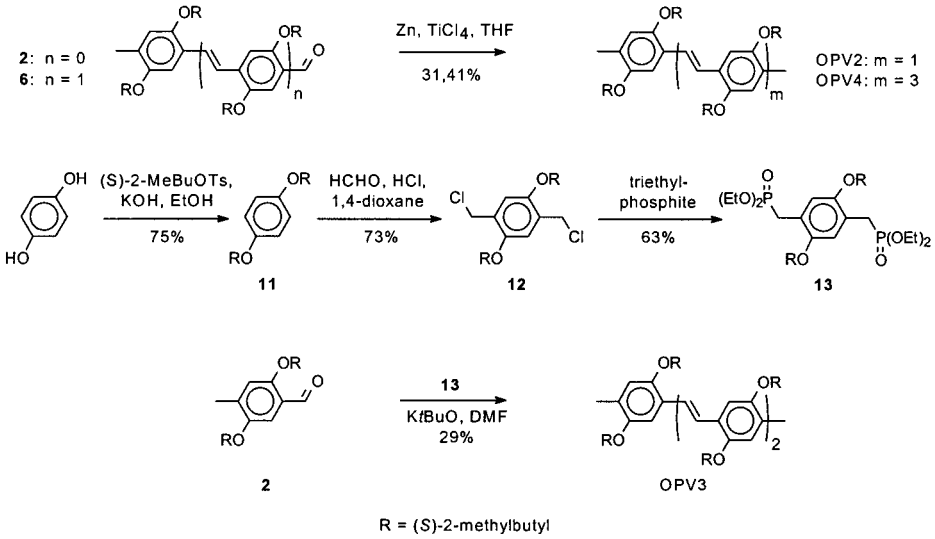

Michaelis−Arbuzov reaction. The Wittig−Horner coupling reaction of **4** with **2** gave compound **5** in a yield of 73% after recrystallization. Bromide **5** was transformed into aldehyde **6** by treatment with *n*-butyllithium and DMF according to the Bouveault method. Pure **6** was isolated in 88% yield after recrystallization. The formylated PPV oligomers **8** and **10** were obtained by repetition of the Wittig−Horner and Bouveault reactions. The relatively low yield of **10** is due to the low solubility of **9** in diethyl ether.

The donor−acceptor dyads OPV*n*-C_{60} were prepared using the well-established Prato reaction[18] (Scheme 2). A chlorobenzene solution of the aldehyde (**2**, **6**, **8**, or **10**), *N*-methylglycine, and C_{60} was stirred for 16 h in the dark at reflux temperature to yield a mixture of C_{60}, the desired monoadducts, and higher adducts. The OPV*n*-C_{60} dyads ($n = 1-4$) were isolated (as mixtures of two diastereomers) after column chromatography in 44, 47, 48, and 40% yields, respectively. Reference compound MP-C_{60} was prepared according to the reported procedure.[19]

The α,ω-dimethyl-oligo(*p*-phenylene vinylene)s with an even number of phenyl rings (OPV2 and OPV4) were prepared by a McMurry homocoupling of the aldehydes **2** and **6** using a reductive mixture of titanium tetrachloride and zinc in tetrahydrofuran (Scheme 3). Pure oligomers were isolated by crystallization in yields of 31 and 41%, respectively. To obtain OPV3, the bisphosphonate compound **13** was synthesized (Scheme 3). Etherification of hydroquinone with enantiomerically pure (*S*)-2-methylbutyl-*p*-toluenesulfonate gave 1,4-bis[(*S*)-2-methylbutoxy]benzene, **11**, in 75% yield. Two-fold chloromethylation of **11** yielded compound **12**, which was subsequently converted to the corresponding bisphosphonate **13**. The double Wittig−Horner reaction of **13** with aldehyde **2** yielded OPV3 in 29% yield after column chromatography.

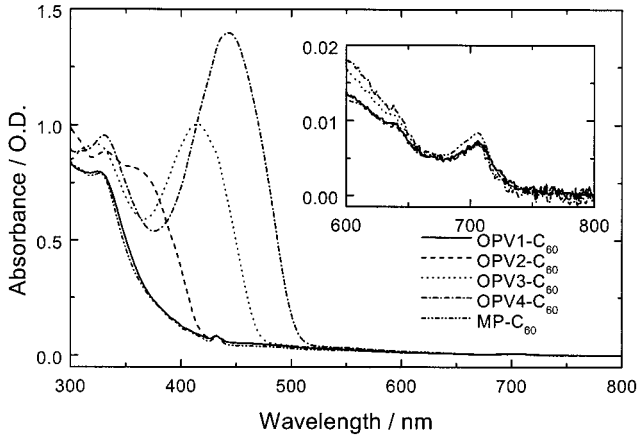

Figure 2. UV/vis spectra of donor−acceptor OPV*n*-C_{60} dyads (1.8×10^{-5} M) and MP-C_{60} in chloroform. The inset shows the spectra in the 600−800 nm range, where the absorption at 703 nm, characteristic of methylfulleropyrrolidines, is observed.

All compounds used in the photophysical investigations were fully characterized using ^{1}H and ^{13}C NMR spectroscopy, mass spectrometry, FT-IR, and elemental analysis.

Ground-State Absorption Spectra. The linear absorption spectra of the OPV*n*-C_{60} dyads in dilute chloroform solution (Figure 2) closely correspond to a superposition of the spectra of the individual donor and acceptor. For a direct comparison, Figure 2 also shows the absorption spectrum of MP-C_{60}, which is almost identical to that of OPV1-C_{60} in the range of 300−800 nm. Very similar spectra were recorded in other solvents, such as toluene and *o*-dichlorobenzene (ODCB). Hence, the covalently linked fullerene and OPV moieties retain the electronic properties of the separate molecules and charge transfer in the ground state does not occur. For all dyads, the

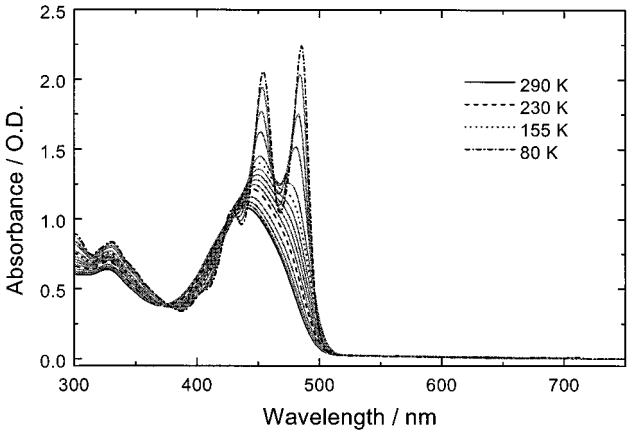

Figure 3. Temperature dependence of the UV/vis absorption of OPV4-C_{60} dissolved in 2-methyltetrahydrofuran recorded in the range from 290 to 80 K by cooling in 15 K steps.

spectra exhibit strong absorptions between 200 and 350 nm and a weak absorption at ~703 nm (inset Figure 2), characteristic of fulleropyrrolidines. For OPV2-C_{60}, OPV3-C_{60}, and OPV4-C_{60}, distinct absorptions are observed at 360, 412, and 438 nm, respectively. These positions are similar to the absorption maxima found in dilute chloroform solutions of OPV2 (357 nm), OPV3 (406 nm), and OPV4 (436 nm), respectively, and are ascribed to the $\pi-\pi^*$ transition of the OPV*n* moieties. The UV/vis spectra demonstrate that it is possible to excite the fullerene moiety selectively at 528 nm (one of the lines available from the Ar-ion laser), because the OPV*n* moieties do not absorb at this wavelength. As a result of the low absorption coefficient of the fulleropyrrolidine in the 440−470 nm region, the OPV4 moiety, and to some extent the OPV3 moiety, can be excited selectively with light of 458 nm. It is not possible to selectively excite either the OPV2 or OPV1 segments without concomitant excitation of the fullerene moiety.

Low-Temperature Absorption Spectra. Figure 3 shows the UV/vis absorption spectra of OPV4-C_{60} in a 2-methyltetrahydrofuran solution between 290 and 80 K. At 290 K, the $\pi-\pi^*$ absorption band of the OPV4 moiety is inhomogeneously broadened with $\lambda_{max} = 439$ nm. With decreasing temperature, the spectra change significantly as the absorption maximum continuously shifts to higher wavelengths. At about 155 K, vibronic fine structure appears in the $\pi-\pi^*$ absorption band. Further cooling results in a significant narrowing of the vibronic features, and at 80 K three to four vibronic bands can be distinguished. At this temperature, the 0−0 transition ($\lambda_{max} = 485$ nm) has gained the highest intensity and the spacing between the vibronic bands is about 1300−1400 cm^{-1}, consistent with a C=C stretch vibration mode.[19] These changes with temperature are interpreted as a gradual loss of conformational disorder because of a planarization of the OPV4 moiety resulting in a larger number of fully planar oligomer chains. In accordance with this geometrical relaxation, we find that the onset of the $\pi-\pi^*$ transition band shifts only slightly with temperature and that the absorption bands characteristic of the rigid fullerene moiety undergo only minor changes with temperature.

Electrochemistry. The cyclic voltammograms of OPV*n*-C_{60} ($n = 1-4$) exhibit one to three quasi-reversible one-electron oxidation waves from the OPV*n* moiety and one reduction wave from the pyrrolidine-bridged C_{60} moiety. Although the first oxidation potential decreases with increasing *n*, the reduction potential remains constant at −0.70 V versus saturated calomel electrode (SCE). The half-wave potentials for the first oxidation and reduction waves of the OPV*n*-C_{60} dyads, OPV*n*'s, and MP-C_{60} are collected in Table 1. The oxidation potentials of the OPV*n*-C_{60} dyads are shifted to slightly higher potentials in comparison with the dimethyl-substituted OPV*n* oligomers. This shift is tentatively ascribed to the different influence of an electron-withdrawing fullerene moiety compared to an electron-donating methyl group.

TABLE 1: Redox Potentials of OPV*n*-C_{60}, OPV*n*, and MP-C_{60} in V vs SCE, As Determined in Dichloromethane

compound	E^0_{red} (V)	E^0_{ox1} (V)	compound	E^0_{red} (V)	E^0_{ox1} (V)
OPV1-C_{60}	−0.70	1.19	OPV2		0.90
OPV2-C_{60}	−0.70	0.97	OPV3		0.80
OPV3-C_{60}	−0.70	0.85	OPV4		0.75
OPV4-C_{60}	−0.70	0.77	MP-C_{60}	−0.70	

Photophysical Studies. Before describing the photoexcitations of the OPV*n*-C_{60} dyads and the OPV*n*/MP-C_{60} mixtures in solution, we briefly discuss the photophysical properties of the individual reference compounds (OPV*n* and MP-C_{60}).

Photoexcitation of OPV*n* in Solution. Recently, we have reported on the singlet and triplet photoexcitations of oligo(*p*-phenylene vinylene)s (OPV*n*'s, $n = 2-7$).[21] The singlet excited state, OPV*n*(S_1), decays radiatively or nonradiatively to the ground state and via intersystem crossing to the OPV*n*(T_1) triplet state. The singlet excited state lifetimes (τ) have been determined for OPV2 ($\tau = 1.80$ ns), OPV3 ($\tau = 1.70$ ns), and OPV4 ($\tau = 1.32$ ns) in toluene solution at room temperature, and there is no significant dependence of τ on the nature of the solvent.[21] The CW-modulated photoinduced absorption (PIA) spectra of OPV3 and OPV4 under matrix-isolated conditions in 2-methyltetrahydrofuran at 100 K exhibit a $T_n \leftarrow T_1$ transition at 2.00 and 2.27 eV for OPV3 and at 1.80 eV for OPV4 with triplet excited state lifetimes of 7.9 and 3.6 ms, respectively.[21] The intensity of the $T_n \leftarrow T_1$ absorptions increases linearly with the pump intensity, consistent with a monomolecular decay mechanism.[21]

Photoexcitation of MP-C_{60} in Solution. Photoexcitation of MP-C_{60} in toluene or ODCB results in weak fluorescence at 1.74 eV and a long-lived triplet excited state. The fluorescence quantum yield in toluene is known to be 6×10^{-4}.[21] Singlet excited state lifetimes of 1.45[15] and 1.28 ns[22] have been reported for toluene solutions. The quantum yield for intersystem crossing from MP-C_{60}(S_1) to MP-C_{60}(T_1) is near unity,[22] and the lifetime of this triplet state is about 200 μs at room temperature.[15] The triplet-state PIA spectrum of MP-C_{60} exhibits a $T_n \leftarrow T_1$ absorption at 1.78 eV with a characteristic shoulder at 1.54 eV.[15] The energy level of the MP-C_{60}(T_1) triplet state has been determined from phosphorescence to be at 1.50 eV above the ground-state level.[22]

Intramolecular Singlet Energy Transfer in OPV*n*-C_{60} Dyads in Toluene. The fluorescence spectra of the OPV*n*-C_{60} ($n = 1$, 2, 3, and 4) dyads, dissolved in toluene, are shown in Figure 4. The spectra were corrected for the Raman scattering of toluene.[23] Although fluorescence from the OPV*n* moieties of the dyads can be observed for $n > 1$, it is quenched by more than 3 orders of magnitude compared to that of the pristine OPV*n* oligomers (Table 2). Apart from the strongly quenched OPV*n* emission, the spectra show a weak fullerene fluorescence of MP-C_{60}(S_1) at 715 nm (Figure 4). The excitation spectra of the fullerene fluorescence coincide with the absorption spectra of the OPV*n*-C_{60} dyads (Figure 5). Surprisingly, the fullerene fluorescence quantum yield in toluene is equal for all four dyads, nearly identical to that of MP-C_{60}, and does not alter with the excitation wavelength. Hence, the fluorescence spectra of OPV*n*-

TABLE 2: Quenching Factors *Q* of the OPV*n* and MP-C_{60} Fluorescence of the OPV*n*-C_{60} Dyads in Toluene and ODCB[a]

	Q_{OPVn} toluene	k_{ET} (s^{-1})	Q_{OPVn} ODCB	$Q_{MP-C_{60}}$ ODCB	k_{CS}^{i} (s^{-1})	k_{CS}^{d} (s^{-1})
OPV2-C_{60}	5200	2.9×10^{12}	8100	5	3.4×10^{9}	1.8×10^{13}
OPV3-C_{60}	3500	2.1×10^{12}	3500	26	1.7×10^{10}	6.3×10^{13}
OPV4-C_{60}	1500	1.1×10^{12}	1900	>50	$>3.4 \times 10^{10}$	$>7.2 \times 10^{13}$

[a] Rate constants for energy transfer (k_{ET}) and charge separation (k_{CS}^{i} and k_{CS}^{d}) as calculated from (1), (3), and (4).

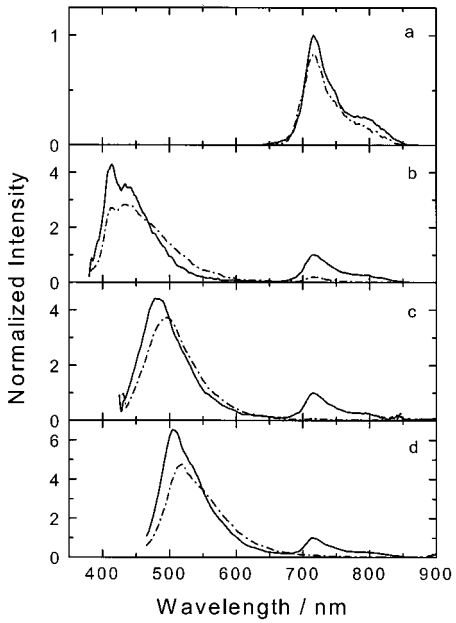

Figure 4. Fluorescence spectra of the OPV*n*-C_{60} dyads in toluene and ODCB, recorded at 295 K: (a) $n = 1$, $\lambda_{ex} = 330$ nm; (b) $n = 2$, $\lambda_{ex} = 366$ nm; (c) $n = 3$, $\lambda_{ex} = 415$ nm; (d) $n = 4$, $\lambda_{ex} = 443$ nm. The fluorescence spectra in toluene (solid lines) were normalized to the fullerene emission at 715 nm. The residual OPV*n* emission for $n = 2-4$ can be seen in the 400−600 nm range. The emission of the OPV*n*-C_{60} dyads in ODCB (dash−dotted lines) is normalized with the same constant as that used for the emission in toluene. A nearly complete quenching of the fullerene emission is observed for $n = 2-4$, whereas the OPV*n* emission decreases only slightly.

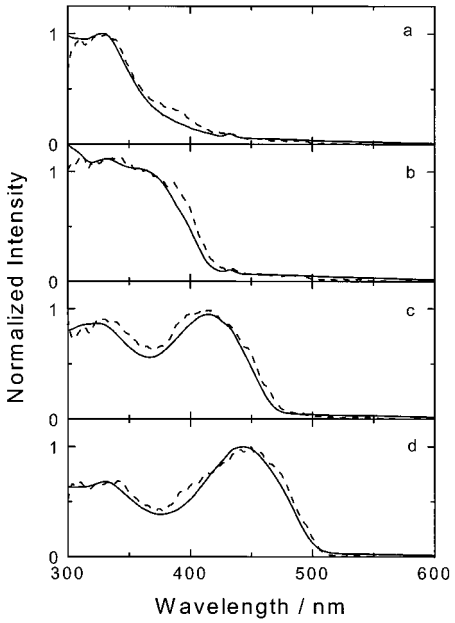

Figure 5. Normalized UV/vis absorption (solid lines) and fluorescence excitation spectra of the fullerene emission at 715 nm (dashed lines) of the OPV*n*-C_{60} dyads in toluene at 295 K: (a) $n = 1$, (b) $n = 2$, (c) $n = 3$, and (d) $n = 4$. In each case, the fluorescence excitation spectrum shows a close correspondence to the absorption spectrum.

C_{60} provide clear evidence for an efficient intramolecular singlet energy transfer from the OPV*n*(S_1) state to the fullerene moiety for $n > 1$.[23]

An estimate for the rate constants of the intramolecular singlet energy transfer (k_{ET}) can be obtained from the extent of quenching of the OPV*n* fluorescence in the dyads and the singlet excited-state lifetime of the OPV*n* oligomers[15] via eq 1.

$$k_{ET} = \frac{Q_{OPVn} - 1}{\tau_{OPVn}} \quad (1)$$

Here, τ_{OPVn} is the lifetime of the singlet excited state of the pristine OPV*n* molecules and Q_{OPVn} is the quenching ratio of the OPV*n* fluorescence of the OPV*n*-C_{60} dyad in comparison with the OPV*n* molecule. The rate constants are collected in Table 2 and indicate that an extremely fast (ca. <1 ps) singlet energy transfer occurs in OPV2-C_{60}, OPV3-C_{60}, and OPV4-C_{60}.

The MP-C_{60}(S_1) state formed via the intramolecular singlet energy transfer in the OPV*n*-C_{60} dyads is expected to decay predominantly via intersystem crossing to the MP-C_{60}(T_1) state, apart from some radiative decay. Consistent with this expectation, the PIA spectrum recorded for all four dyads in toluene solution shows the characteristic MP-C_{60} $T_n \leftarrow T_1$ absorption at 1.78 eV with a shoulder at 1.54 eV (Figure 6a). The PIA bands increase in a nearly linear fashion with the excitation intensity ($-\Delta T \propto I^p$, $p = 0.80-1.00$) consistent with a monomolecular decay mechanism, but it should be noted that bimolecular mechanisms such as the quenching of the MP-C_{60}-(T_1) state by molecular oxygen would also give the same behavior. The lifetime of the triplet state is in the range of 140−280 μs.

The observations from fluorescence and PIA spectra provide strong evidence that in toluene the OPV*n* moieties of the OPV*n*-C_{60} dyads with $n > 1$ serve as an antenna system to funnel the excitation energy to the fullerene moiety.[24]

Intermolecular Triplet Energy Transfer in OPV*n*/MP-C_{60} Mixtures in Toluene. The photophysical processes change dramatically when mixtures of MP-C_{60} and OPV*n* in toluene are excited instead of the covalently bound OPV*n*-C_{60} dyads. Although intermolecular energy transfer from singlet excited oligo(*p*-phenylene vinylene)s to MP-C_{60} is energetically possible in OPV*n*/MP-C_{60} mixtures, it is less likely to occur because such transfer is limited by diffusion and the nanosecond lifetime of the singlet excited state. Hence, the OPV*n*(S_1) state in these mixtures will decay via fluorescence and intersystem crossing to the OPV*n*(T_1) state. The PIA spectrum of MP-C_{60} and OPV4 (1:1 molar ratio) in toluene, recorded upon selective excitation of OPV4 at 458 nm, exhibits a band at 1.80 eV with a weak shoulder at 1.52 eV (Figure 7). The PIA signal in the high-energy region is obscured by the extremely intense OPV4 fluorescence in the region from 1.85 to 2.5 eV, which could only be partially corrected. The negative $-\Delta T/T$ above 2 eV is an artifact caused by this correction. A monomolecular decay mechanism is inferred from the intensity dependence of the 1.80 eV PIA band ($-\Delta T \propto I^p$, $p = 0.89-0.92$). A lifetime of ~200

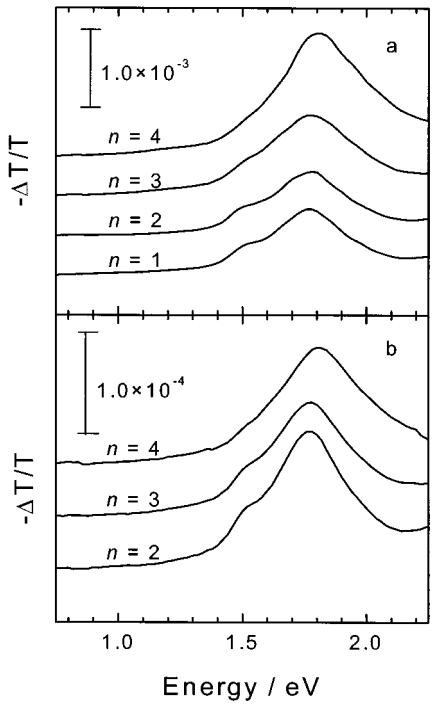

Figure 6. (a) PIA spectra of OPV*n*-C_{60} dyads (4×10^{-4} M) in toluene at 295 K, recorded with excitation at 351.3 and 363.8 nm for $n = 1$ and 2 and at 457.9 nm for $n = 3$ and 4. (b) PIA spectra of OPV*n* (4×10^{-4} M) codissolved with MP-C_{60} (4×10^{-4} M) in toluene at 295 K with excitation at 528 nm.

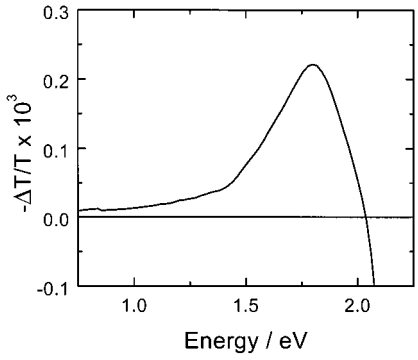

Figure 7. PIA spectra of OPV4 (4×10^{-4} M) codissolved with MP-C_{60} (4×10^{-4} M) in toluene at 295 K recorded with excitation at 457.9 nm.

μs was determined by varying the modulation frequency between 30 and 3800 Hz. The spectral features and the lifetime are characteristic for the MP-$C_{60}(T_1)$ state. They do not coincide with the PIA spectrum recorded for OPV4, which shows a maximum at 1.80 eV, without any shoulder to lower energy.[21] The observation of the MP-$C_{60}(T_1)$ spectrum and, hence, the quenching of the OPV4(T_1) state indicate that after intersystem crossing an efficient intermolecular triplet energy transfer occurs from the OPV4(T_1) state to MP-C_{60}, generating the MP-C_{60}-(T_1) state. Because the photogenerated OPV4(T_1) state is quenched by the presence of MP-C_{60}, we conclude that the triplet state energy of OPV4 is higher than 1.50 eV, the triplet state energy of MP-C_{60}. Because shorter oligo(*p*-phenylene vinylene)s are expected to have an even higher triplet level, we can conclude that the fullerene triplet level corresponds to the lowest excited state in toluene for all dyads studied here.

Consistently, the PIA spectra of toluene solutions containing MP-C_{60} and OPV*n* ($n = 2$, 3, or 4) in a 1:1 molar ratio, recorded using selective photoexcitation of MP-C_{60} at 528 nm (Figure 6b), exhibit an absorption at 1.78 eV with an associated shoulder at 1.54 eV, characteristic of MP-$C_{60}(T_1)$.[15] The monomolecular decay ($-\Delta T \propto I^p$, $p = 0.89-0.96$) and lifetime of 150−260 μs associated with these PIA bands support this assignment. Furthermore, weak fullerene fluorescence at 1.73 eV (715 nm) is observed under these conditions for all three mixtures. No characteristic PIA bands of OPV$n^{+\bullet}$ radical cations or MP-$C_{60}^{-\bullet}$ radical anions are discernible under these conditions. From these observations, we conclude that electron transfer from the ground state of the OPV*n* molecules to the singlet or triplet excited state of MP-C_{60} does not occur in toluene solution.

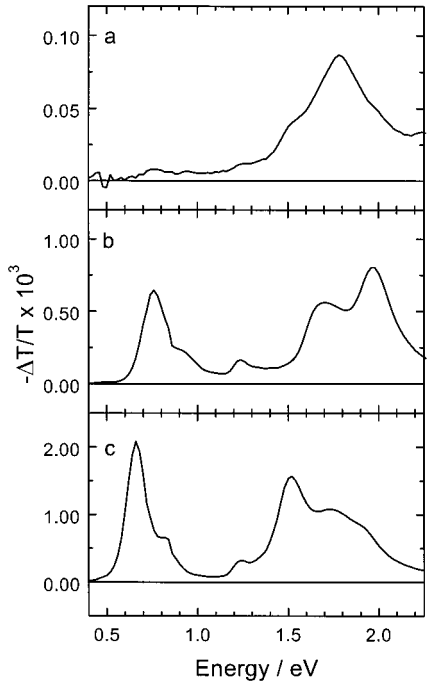

Figure 8. PIA spectra of OPV*n* (4×10^{-4} M) codissolved with MP-C_{60} (4×10^{-4} M) in ODCB at 295 K recorded with excitation at 528 nm: (a) OPV2/MP-C_{60}, (b) OPV3/MP-C_{60}, and (c) OPV4/MP-C_{60}.

Intermolecular Electron Transfer in OPV*n*/MP-C_{60} Mixtures in *o*-Dichlorobenzene. The dielectric constant (permittivity) of ODCB ($\epsilon = 9.93$) is significantly higher than that of toluene ($\epsilon = 2.38$). Photoinduced electron transfer will be more favored in this more polar solvent because the Coulombic attraction between the resulting opposite charges is more screened and the charged ions are better solvated than in toluene. Indeed, the PIA spectra of 1:1 molar mixtures of MP-C_{60} and OPV4 or OPV3 in ODCB give direct spectral evidence for intermolecular photoinduced electron transfer. For both mixtures, an intense PIA spectrum of the charge-separated state was observed after selective excitation of MP-C_{60} at 528 nm (Figure 8b,c). Strong absorptions for the OPV4$^{+\bullet}$ (0.66, 1.52, and 1.73 eV) and OPV3$^{+\bullet}$ (0.77, 1.70, and 1.97 eV) radical cations were observed, together with the characteristic absorption band of the MP-$C_{60}^{-\bullet}$ radical anion at 1.24 eV. For each PIA band, the change in transmission as a function of the modulation frequency was recorded and fitted to the expression for bimolecular decay, resulting in estimates for the charge-separated state lifetime of 2.5−3.1 ms for OPV4$^{+\bullet}$/MP-$C_{60}^{-\bullet}$ and 4.1−4.7 ms for OPV3$^{+\bullet}$/MP-$C_{60}^{-\bullet}$, respectively. Increasing the pump beam intensity resulted in a nonlinear increase of the absorption intensities ($-\Delta T \propto I^p$, $p = 0.62-0.71$). Although for bimolecular decay a square-root intensity dependence of the PIA signal is often observed, it is noticeable that the pump intensity dependence of the PIA signal becomes linear when the modulation frequency

is much larger than the inverse bimolecular lifetime.[25] In the present case with $\omega = 275$ Hz and $\tau \approx 2-5$ ms, both are of the same magnitude and an intermediate value can be expected. Therefore, we conclude that the results are consistent with bimolecular decay and, hence, with intermolecular recombination of positive and negative charges. Because MP-C_{60} is initially excited, we attribute the formation of radical ions to an intermolecular electron transfer between ground-state OPV3 or OPV4 as a donor and the triplet state of MP-C_{60} as an acceptor.[26]

The PIA spectra of the mixture of OPV2 and MP-C_{60} in ODCB, recorded with selective excitation of MP-C_{60} at 528 nm (Figure 8a), exhibits the transitions of the MP-$C_{60}(T_1)$ state at 1.78 and 1.54 eV. These bands increase linearly with the excitation intensity ($-\Delta T \propto I^p$, $p = 0.99-1.00$) and correspond to a lifetime of 170−290 μs. Together with the concurrent absence of polaron absorptions, we infer that intermolecular charge transfer between OPV2 and MP-C_{60} does not occur in ODCB.[27]

Intramolecular Electron Transfer in OPV*n*-C_{60} Dyads in *o*-Dichlorobenzene. Figure 4 shows the Raman corrected emission spectra of the OPV*n*-C_{60} dyads in ODCB obtained upon (near) selective photoexcitation of the OPV moiety. Similar to solutions in toluene, the fluorescence of the OPV*n* moiety of the dyads is strongly quenched compared to the fluorescence of the pristine OPV*n* in ODCB. The quenching ratios, Q_{OPVn}, collected in Table 2, are somewhat larger than those in toluene. The most dramatic difference between the fluorescence spectra of the OPV*n*-C_{60} dyads recorded in the two different solvents, however, is the strong quenching of the fullerene emission at 715 nm for solutions of OPV2-C_{60}, OPV3-C_{60}, and OPV4-C_{60} in ODCB but not for OPV1-C_{60}. The fullerene quenching ratio, $Q_{C_{60}}$, calculated with respect to the fluorescence of MP-C_{60} in ODCB, increases with conjugation length of the OPV*n* moiety from approximately 5 for OPV2-C_{60} to 26 for OPV3-C_{60} to more than 50 for OPV4-C_{60} (Table 2). The quenching of the fullerene emission in the dyads may result from either an ultrafast process that quenches the initially formed OPV*n*(S_1) state or a rapid relaxation of the MP-$C_{60}(S_1)$ state, once this is formed via energy transfer. The experimental observation that the residual OPV*n* fluorescence of the OPV*n*-C_{60} dyads in ODCB is comparable to that in toluene gives support to the latter explanation.

Intramolecular charge separation is energetically favored over intermolecular charge separation because the spatial separation of charges, and hence the Coulombic term, is limited by the fixed distance between donor and acceptor within the covalent donor−acceptor dyad. Because intermolecular photoinduced electron transfer occurs in mixtures of MP-C_{60} and OPV4 or OPV3 in ODCB, we may expect that intramolecular photoinduced electron transfer occurs in the corresponding OPV3-C_{60} and OPV4-C_{60} dyads in ODCB as well. The lifetime of an intramolecularly charge-separated state in molecular donor-fullerene dyads, however, usually does not extend into the microsecond regime but is limited to the low nanosecond time domain.[10] For cases in which the donor is separated from the fullerene by a long rigid bridge[28,29] or the donor has a low oxidation potential (e.g., tetrathiafulvalene or ferrocene),[30−32] the lifetime of the charge-separated state was found to be in the microsecond range. In general, excited states with a lifetime $\tau \leq \sim 10$ μs cannot be detected with the CW-modulated PIA technique because the steady-state concentration that is achieved in the modulated experiment is below the detection limit ($\Delta T/T \approx 10^{-6}$). Therefore, it is surprising to see that the PIA spectra of OPV3-C_{60} and OPV4-C_{60} dissolved in ODCB exhibit the characteristic absorptions of a charge-separated state (Figure 9c,d). Although the intensities of the OPV$n^{+\bullet}$ radical cation and MP-$C_{60}^{-\bullet}$ radical anion absorptions are significantly lower in comparison with the PIA signals observed for mixtures of OPV*n* and MP-C_{60} in ODCB, the characteristic features are evident. Remarkably, lifetimes up to 20 ms can be observed for these charge-separated states. In view of the expected (sub)nanosecond lifetime,[10] we consider this extremely long lifetime to be incompatible with an intramolecular charge-separated state and attribute the signals to an intermolecular charge-separated state. This intermolecular charge-separated state is formed either by direct charge transfer between singlet excited OPV*n*-$C_{60}(S_1)$ and a second dyad in the ground state or by charge transfer from the short-lived intramolecular charge-separated OPV$n^{+\bullet}$-$C_{60}^{-\bullet}$ state to a neutral OPV*n*-C_{60} dyad, resulting in separate OPV$n^{+\bullet}$-C_{60} and OPV*n*-$C_{60}^{-\bullet}$ radical ions. The longer lifetime as compared to OPV*n*/MP-C_{60} ($n = 3$ or 4) mixtures is due to the lower concentration of the OPV$n^{+\bullet}$-C_{60} and OPV*n*-$C_{60}^{-\bullet}$ radical ions and, hence, the reduced bimolecular decay rate.

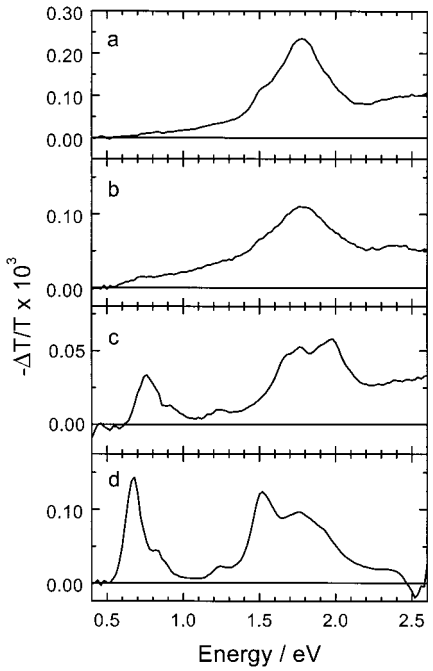

Figure 9. PIA spectra of the OPV*n*-C_{60} dyads in ODCB (4×10^{-4} M) at 295 K for (a) $n = 1$, (b) $n = 2$, (c) $n = 3$, and (d) $n = 4$. The spectra were recorded with excitation at 351.1 and 363.8 nm for $n = 1$ and 2 and at 457.9 nm for $n = 3$ and 4.

Photoexcitation of OPV2-C_{60} in ODCB leads to seemingly contradictory observations: although the fullerene emission is partly quenched (Figure 4, Table 2), consistent with electron transfer, the MP-$C_{60}(T_1)$ state is observed in the PIA spectrum (Figure 9b), indicating a combination of energy transfer and intersystem crossing. The result can be rationalized as follows; if the energy level of the lowest lying neutral excited state, OPV2-$C_{60}(T_1)$, is close to the energy level of the intramolecular charge-separated state, energy and electron transfer will occur simultaneously. The likelihood of this degeneracy will be demonstrated in the section on energetics of charge transfer.

The PIA spectrum of OPV1-C_{60} in ODCB shows the absorption of the fullerene triplet state (Figure 9a), and no significant quenching of the fullerene emission is observed (Figure 4a). Both observations are consistent with the absence of an intramolecular photoinduced electron transfer in OPV1-C_{60}, which can be rationalized by the high oxidation potential of the OPV1 moiety.

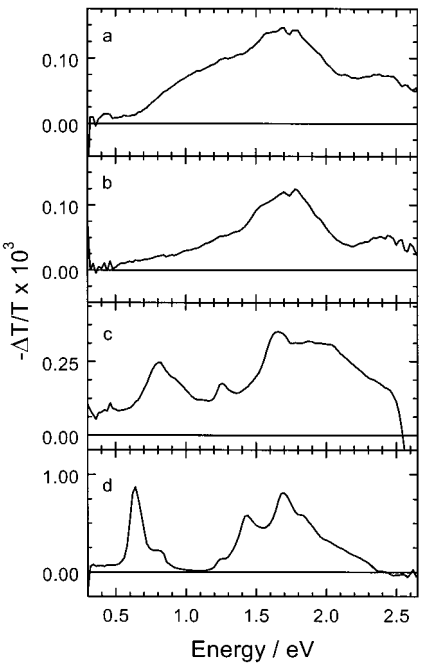

Figure 10. PIA spectra of OPV*n*-C_{60} thin films on quartz: (a) $n = 1$, (b) $n = 2$, (c) $n = 3$, and (d) $n = 4$. The spectra were recorded at 80 K by exciting at 351.1 and 363.8 nm for $n = 1$ and 2 and at 457.9 nm for $n = 3$ and 4 with 25 mW and a modulation frequency of 275 Hz.

Photoinduced Electron Transfer of OPV*n*-C_{60} in Thin Films. Thin films of OPV*n*-C_{60} ($n = 1-4$) were prepared by casting from solution onto quartz substrates. For OPV1-C_{60} and OPV2-C_{60}, the PIA spectra of the thin films recorded at 80 K with excitation at 351 and 363 nm are similar (Figure 10a,b). In both spectra, a broad low-intensity absorption is discernible between 1.0 and 2.2 eV, with a maximum at about 1.72 eV. The exact origin of the broad band is presently not known. The spectrum shows some similarity to that of the MP-$C_{60}(T_1)$ state in solution, and the two characteristic absorption bands of oligo(*p*-phenylene vinylene) radical ions are absent. Therefore, we tentatively assign the spectra (at least in part) to triplet−triplet absorptions of the fullerene moiety. The lifetime of the MP-$C_{60}(T_1)$ state, as derived from modulation frequency dependency measurements, is ∼230 μs for OPV1-C_{60} and ∼275 μs for OPV2-C_{60}. These spectral characteristics suggest that photoinduced electron transfer does not occur (or occurs only to a small extent) in thin films of OPV1-C_{60} and OPV2-C_{60}.

The PIA spectra of thin films of OPV3-C_{60} and OPV4-C_{60} recorded with excitation at 458 nm differ dramatically from those of OPV1-C_{60} and OPV2-C_{60} (Figure 10c,d). For OPV3-C_{60} and OPV4-C_{60}, the characteristic absorption band of the MP-$C_{60}^{-\bullet}$ radical anion is observed at 1.25 eV. Furthermore, the spectra show absorptions for the $OPV3^{+\bullet}$ and $OPV4^{+\bullet}$ radical cations at 0.82 and 1.66 eV ($OPV3^{+\bullet}$) and at 0.64, 1.44, and 1.70 eV ($OPV4^{+\bullet}$). These observations give direct spectral evidence for photoinduced electron transfer. The intensity of the PIA bands increases approximately with the square-root of the pump intensity ($-\Delta T \propto I^p$, $p = 0.46-0.57$ for OPV3-C_{60} and $p = 0.36-0.50$ for OPV4-C_{60}). This square-root intensity dependency indicates a bimolecular decay mechanism, consistent with the recombination of positive and negative charges. Varying the modulation frequency from 30 to 3800 Hz results in a continuous decrease of the intensity of the PIA bands of OPV3-C_{60} and OPV4-C_{60}, indicating a distribution of lifetimes. The average lifetime of the charge-separated states in thin films of OPV3-C_{60} and OPV4-C_{60} is on the order of 0.5−1.5 ms. This long lifetime in the films is in strong contrast with the short lifetime of the intramolecular charge-separated state as inferred from the experiments in ODCB. Typically, the lifetime of an intramolecular charge-separated state in fullerene-containing dyads and triads is in the (sub)nanosecond time scale,[10] although a few examples are known with a lifetime in the microsecond domain.[28−32] Therefore, we propose that the long lifetimes in the film are due to migration of the hole and/or the electron to other molecules in the film, after the photoinduced electron transfer.[33] The resulting intermolecular charge-separated state can no longer decay via the fast geminate intramolecular back electron transfer and will therefore have an increased lifetime. At present, we have no indication that an initially formed intramolecular charge transfer facilitates the formation of the long-lived intermolecular charge-separated state.

Photovoltaic Devices of OPV4-C_{60}. The increased lifetime of the charge-separated state in the solid state, resulting from the migration of opposite charges to different molecules, extends into the millisecond time domain similar to that of polymer−fullerene composite films.[1,5] This opens the possibility of utilizing the OPV*n*-C_{60} dyads as the active material in a photovoltaic device similar to that using the blends. As an important difference with previous bulkheterojunction cells,[6,7] the covalent linkage between donor and acceptor in these molecular dyads restricts the dimensions of the phase separation between the oligomer and the fullerene that could freely occur in blends of the individual components. Through a link of the donor and acceptor via a covalent bond, a predefined phase segregation of nanoscopic dimension could possibly be created that would give rise to a well-ordered bicontinuous interpenetrating network of both donor and acceptor. The nanoscopic dimension of the phase separation is advantageous because the exciton diffusion length in conjugated polymers is limited to that length scale. Molecular ordering will enhance the charge carrier mobility and hence the separation of photogenerated electrons and holes. Finally, the bicontinuous network will ensure the unrestricted transport of electrons and holes to the electrodes. Each of these three factors, generation, stabilization, and transport, may improve the efficiency of photovoltaic cells. The OPV*n*-C_{60} dyads can be considered as a primitive attempt to obtain more ordered and well-defined phase-separated D−A networks.

To test the applicability of the molecular dyads for light energy conversion, we have prepared photovoltaic devices in which OPV4-C_{60} is sandwiched between aluminum and polyethylenedioxythiophene polystyrenesulfonate (PEDOT−PSS)-covered indium−tin oxide (ITO) electrodes. Figure 11 shows the semilogarithmic plot of the *I*/*V* curves of a typical device in the dark and under white-light illumination of a halogen lamp at ∼65 mW cm^{-2}. The *I*/*V* curves are completely reversible, and the device shows diode behavior with a rectification ratio between −2 and +2 V of approximately 100, which shows that the device has few or no shunts. In the dark, a small kink is discernible in the semilogarithmic plot of the *I*/*V* curve between 0 and 1 V, representing the small ohmic contribution from the shunt resistance. Under ∼65 mW cm^{-2} white-light illumination, a short-circuit current (I_{sc}) of 235 μA cm^{-2} and an open-circuit voltage (V_{oc}) of 650 mV are observed for this device. The fill factor (FF), defined as $(I_{max} \times V_{max})/(I_{sc} \times V_{oc})$ with I_{max} and V_{max} corresponding to the point of maximum power output, is 0.25. The relatively low FF can be explained by recombination of charge carriers either in the bulk or at the electrode interfaces. Because the photocurrent was found to be linear with the light intensity, we rule out bimolecular recombination and suggest

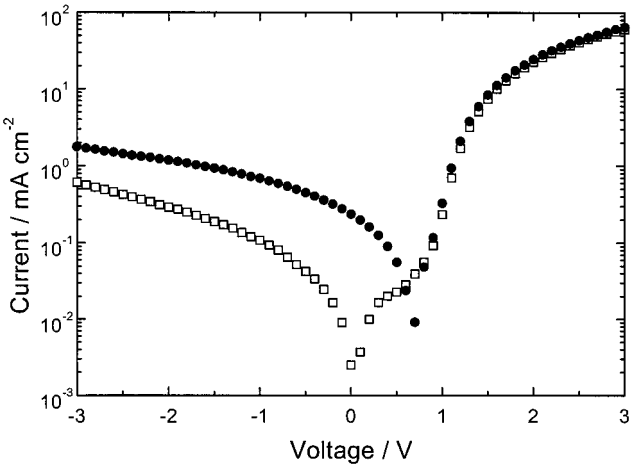

Figure 11. Semilogarithmic plot of the current/voltage curves of a PET/ITO/PEDOT−PSS/OPV4-C_{60}/Al photovoltaic cell in which OPV4-C_{60} is the active material. Open squares represent the dark curve, and solid squares represent data recorded under ~65 mW cm^{-2} white-light illumination.

surface recombination as a possible mechanism for the low FF. Because aluminum is known to give rather good ohmic contacts in bulk heterojunction cells,[34] we suggest surface recombination at the ITO electrode as the likely cause of the low FF. The present values of I_{sc} and V_{oc} are significantly enhanced in comparison with the device characteristics of a related oligo(*p*-phenylene vinylene)-C_{60} dyad[14] and are quite similar to those previously reported for π-conjugated polymer/fullerene solar cells,[35] although there has been considerable progress in energy conversion efficiencies of these devices recently.[36] The results indicate that indeed a bicontinuous network of the donor and acceptor moieties is formed in a film of OPV4-C_{60}. Two factors limit the intrinsic efficiency of the OPV4-C_{60}-based device, compared to that of the corresponding poly(*p*-phenylene vinylene)/fullerene blends. First, the absorption spectrum of the OPV4 oligomer does not cover the wavelength range of the corresponding polymer because of the reduced conjugation length. Second, the intrinsic fullerene/OPV weight ratio of 0.71 in OPV4-C_{60} is significantly lower than the optimized fullerene/polymer weight ratio of 4, presently used in the most efficient polymer solar cells.[3]

Energetic Considerations for Energy and Electron Transfer. To rationalize the observed differentiation between energy and electron transfer by the photoexcited OPV*n*-C_{60} dyads in apolar and polar solvents, we calculated the change in free energy for charge separation (ΔG_{cs}) using the Weller equation:[17]

$$\Delta G_{cs} = e(E_{ox}(\mathrm{D}) - \mathrm{E}_{red}(\mathrm{A})) - E_{00} - \frac{e^2}{4\pi\epsilon_0\epsilon R_{cc}} - \frac{e^2}{8\pi\epsilon_0}\left(\frac{1}{r^+} + \frac{1}{r^-}\right)\left(\frac{1}{\epsilon_{ref}} - \frac{1}{\epsilon_{ref}}\right) \quad (2)$$

In this equation, $E_{ox}(\mathrm{D})$ and $E_{red}(\mathrm{A})$ are the oxidation and reduction potentials of the donor and acceptor molecules or moieties measured in a solvent with relative permittivity ϵ_{ref}, E_{00} is the energy of the excited state from which the electron transfer occurs, and R_{cc} is the center-to-center distance of the positive and negative charges in the charge-separated state. The radii of the positive and negative ions are given by r^+ and r^-, and ϵ_s is the relative permittivity of the solvent; $-e$ is the electron charge, and ϵ_0 is the vacuum permittivity.

TABLE 3: Center-to-Center Distance (R_{cc}) of Donor and Acceptor in OPV*n*-C_{60} Dyads, Radius (r^+) of OPV*n* Radical Cation, Energy of OPV*n*(S_1) State, and Free Energies of Intramolecular (G_{cs}) and Intermolecular (G_{cs}^{∞}) Charge-Separated States in OPV*n*-C_{60} Dyads and OPV*n*/MP-C_{60} Mixtures Calculated from (2)

	R_{cc} (Å)	r^+ (Å)	$E_{OPVn(S1)}$ (eV)	solvent	G_{cs} (eV)	G_{cs} (eV)
OPV1-C_{60}	7.0	3.3	4.77	toluene	2.10	
				ODCB	1.64	
OPV2-C_{60}	9.5	4.0	3.03	toluene	1.99	2.56
				ODCB	1.48	1.56
OPV3-C_{60}	12.3	4.6	2.64	toluene	1.94	2.38
				ODCB	1.40	1.47
OPV4-C_{60}	15.3	5.1	2.44	toluene	1.91	2.29
				ODCB	1.34	1.42

For OPV*n*-C_{60} and mixtures of OPV*n* and MP-C_{60} in solution, E_{ox} and E_{red} were determined via cyclic voltammetry in dichloromethane ($\epsilon = 8.93$) (Table 1). The R_{cc} distances (Table 3) in the dyads were determined by molecular modeling, assuming that the charges are located at the centers of the OPV and fullerene moieties. For intermolecular charge transfer, the value of R_{cc} was set to infinity. The radius of the negative ion of C_{60} was set to $r^- = 5.6$ Å, based on the density of C_{60}.[28] To estimate the radii for the positive ions (a radius being a substantial simplification for the one-dimensionally extended conjugated OPV moieties!), we used the van der Waals volume of OPV molecules, ignoring the 2-methylbutoxy side chains because the positive charge will be confined to the conjugated segment. For stilbene, an experimental value of $r^+ = 3.96$ Å can be obtained from the density ($\rho = 1.159$ g cm^{-3}), derived from the X-ray crystallographic data,[37] via $r^+ = [3M/(4\pi\rho N_A)]^{1/3}$. For the other oligomers, no crystallographic data are available and we calculated the van der Waals volumes of benzene, stilbene, 1,4-distyrylbenzene, and 4,4′-distyrylstilbene using Macromodel and a MM2 force field. After correction for 26% free-volume in a close packing of spheres, the values collected in Table 3 were obtained. The experimental and theoretical values for stilbene are in close agreement. With these approximations, the free energies of the intramolecular ($G_{cs} = \Delta G_{cs} + E_{00}$) and intermolecular ($G_{cs}^{\infty} = \Delta G_{cs}^{\infty} + E_{00}$) charge-separated states have been calculated (Table 3), and the relative ordering of the states is depicted in Figure 12.

From Figure 12b and Table 3, it is clear that the intramolecular charge-separated state is energetically located below the OPV*n*(S_1) state in both solvents and for each *n*. However, in toluene all charge-separated states are higher in energy than the MP-C_{60}(S_1) and MP-C_{60}(T_1) states, which are located at 1.74 and 1.50 eV, respectively. In ODCB, the situation changes dramatically; the energy of the intramolecular charge-separated state drops below that of the MP-C_{60}(S_1) state for each *n* and even drops below that of the corresponding MP-C_{60}(T_1) state except for $n = 1$, indicating that electron transfer will result in a gain of free energy for $n > 1$. In fact, the predictions based on eq 2 (Table 3) are in excellent agreement with the quenching of the MP-C_{60}(S_1) fluorescence, as shown in Figure 4, which occurs for $n > 1$. For the intermolecular charge-separated states, the relevant state for comparison is the MP-C_{60}(T_1) state only, because these charge-separated states are formed via the triplet manifold. Table 3 and Figure 12a show that intermolecular electron transfer is energetically favored in ODCB for OPV3 and OPV4 but not for OPV2,[38] again in full agreement with the experimental results inferred from PIA spectroscopy (Figure 8).

The close correspondence of experimental results with the relative ordering of the various excited states as derived from

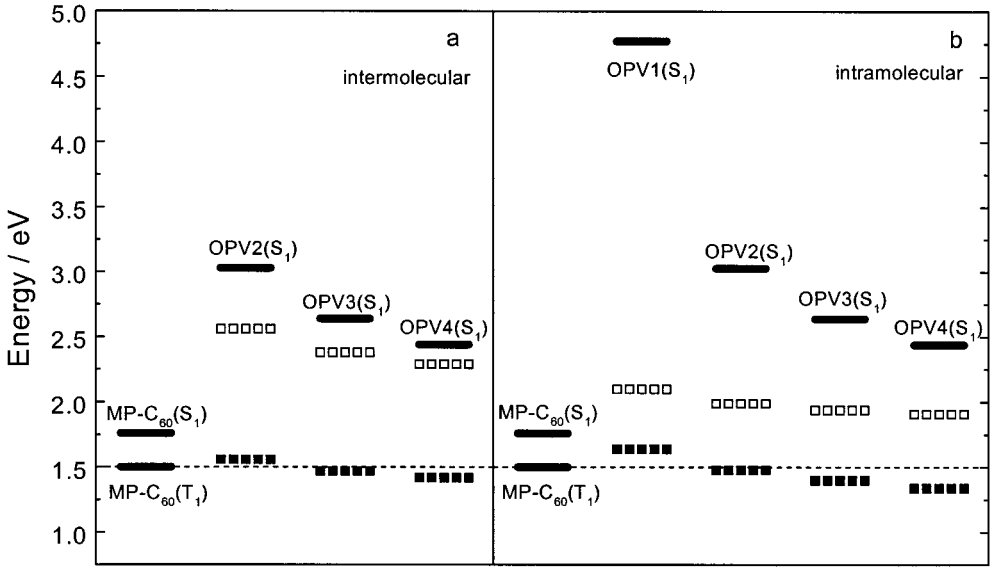

Figure 12. Excited-state energy levels. The singlet (S_1) energy levels of OPV*n* and MP-C_{60} (solid bars) were determined from fluorescence data. The MP-C_{60}(T_1) level (solid bar and dashed line) was taken from literature phosphorescence data.[22] The levels of the charge-separated states for (a) intermolecular charge transfer in OPV *n*/MP-C_{60} mixtures and (b) intramolecular charge transfer in OPV*n*-C_{60} dyads were determined using eq 2 (see text and Table 3). The open squares are for toluene, and the solid squares are for ODCB.

eq 2 shows the strength of this approach in explaining the discrimination between photoinduced energy and charge transfer in conjugated oligomer−fullerene dyads.

Kinetics of Energy and Electron Transfer. A semiquantitative estimate for the rate constants of the various photophysical processes can be obtained from the fluorescence quenching. On the basis of the quenching ratios of the OPV fluorescence and the OPV*n* singlet excited state lifetimes, the rate constants for energy transfer reactions in toluene solutions were estimated to be 2.9×10^{12}, 2.1×10^{12}, and 1.1×10^{12} s^{-1} for OPV2-C_{60}, OPV3-C_{60}, and OPV4-C_{60}, respectively (Table 2). We assume that similar rate constants for energy transfer will apply to ODCB solutions because the energy level and the lifetime of the singlet excited states are not strongly affected by the polarity of the solvent.[21] For OPV2-C_{60}, OPV3-C_{60}, and OPV4-C_{60}, intramolecular photoinduced electron transfer is observed in ODCB, as evidenced by the quenching of the MP-C_{60}(S_1) fluorescence. In principle, electron transfer can take place either directly from the initially formed OPV*n*(S_1) state or indirectly, in a two-step process, via the MP-C_{60}(S_1) state (Figure 13). For indirect photoinduced electron transfer, that is, after singlet energy transfer to MP-C_{60}, the rate constant (k_{cs}^{i}) is given by eq 3.

$$k_{cs}^{\,i} = \frac{Q_{C_{60}} - 1}{\tau_{C_{60}}} \tag{3}$$

Here, $Q_{C_{60}}$ is the quenching ratio of the fullerene emission of the OPV*n*-C_{60} dyads in ODCB in comparison with MP-C_{60}, and $\tau_{C_{60}}$ is the lifetime of the singlet excited state of MP-C_{60} (1.45 ns).[15] The values for k_{cs}^{i} in Table 2 show that the electron transfer from the MP-C_{60}(S_1) state occurs in the time scale of ∼60 ps for OPV3-C_{60} and ∼30 ps for OPV4-C_{60} but is much slower for OPV2-C_{60} (∼290 ps). If a direct electron transfer from the OPV*n*(S_1) state occurred, the decrease in fullerene emission would necessarily result from a quenching of the OPV*n*(S_1) state, because it would be faster than the energy

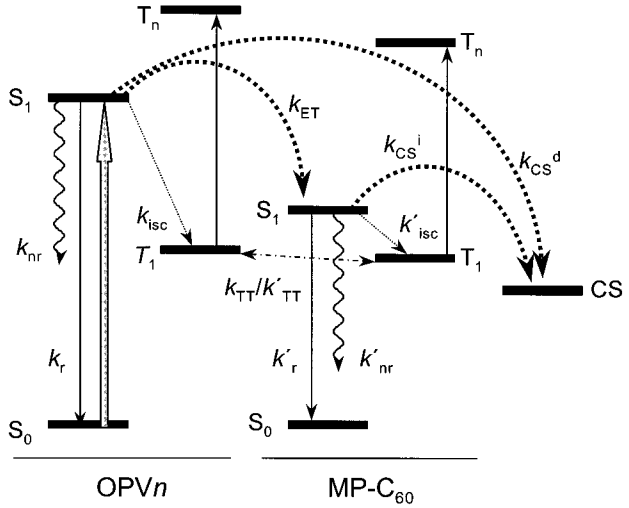

Figure 13. Schematic diagram describing energy levels of singlet (S_0 and S_1), triplet (T_1 and T_n), and charge-separated (CS) states of OPV*n*-C_{60} dyads. The energy transfer (k_{ET}) and the indirect (k_{CS}^{i}) and direct (k_{CS}^{d}) charge-separation processes are indicated with the curved dotted arrows. The solid arrow describes the initial excitation of the OPV*n* moiety. Other symbols are k_r and k'_r for the radiative rate constants, k_{nr} and k'_{nr} for the nonradiative decay constants, k_{isc} and k'_{isc} for the intersystem crossing rate constants, and k_T and k'_{TT} for the rate constants for triplet-energy transfer, each for OPV*n* and MP-C_{60}, respectively.

transfer reaction. In this case, the rate constant (k_{cs}^{d}) for electron transfer can be derived from

$$k_{cs}^{\,d} = \frac{(Q_{OPVn} - 1)(Q_{C_{60}} - 1)}{\tau_{OPVn}} \tag{4}$$

The calculated values of k_{cs}^{d} (Table 2) indicate that direct intramolecular electron transfer would have to be extremely fast, especially for OPV3 and OVP4 (14−20 fs). Moreover, if direct electron transfer occurred, an additional quenching of the residual OPV*n* emission must be expected. However, Figure 4 shows that there is no significant additional quenching of the

TABLE 4: Reorganization Energy (λ), Free-Energy Change (ΔG_{cs}), and Barrier ($\Delta G^{\ddagger}_{cs}$) for Intramolecular Electron Transfer in OPV*n*-C_{60} Dyads in Different Solvents Relative to the Energies of the OPV*n*(S_1) and MP-C_{60}(S_1) States, As Calculated from (2), (5), and (6)

			OPV*n*(S_1)		MP-C_{60}(S_1)	
compound	solvent	λ (eV)	ΔG_{cs} (eV)	$\Delta G^{\ddagger}_{cs}$ (eV)	ΔG_{cs} (eV)	$\Delta G^{\ddagger}_{cs}$ (eV)
OPV2-C_{60}	toluene	0.34	−1.04	0.36	0.23	0.24
	ODCB	0.80	−1.55	0.18	−0.28	0.09
OPV3-C_{60}	toluene	0.34	−0.71	0.09	0.18	0.20
	ODCB	0.83	−1.24	0.05	−0.36	0.07
OPV4-C_{60}	toluene	0.35	−0.53	0.02	0.15	0.18
	ODCB	0.86	−1.10	0.02	−0.42	0.06

OPV*n* emission in ODCB in comparison with the quenching already achieved by energy transfer in toluene. Hence, the fluorescence quenching experiments strongly suggest that photoinduced electron transfer in the OPV*n*-C_{60} dyads in ODCB solution is a two-step process when the OPV*n* is excited initially, involving singlet energy transfer prior to charge separation.[26]

The Activation Barrier for Charge Separation. Further insight into the kinetics of charge separation can be obtained from the activation barrier of charge separation. The Marcus equation provides an estimate for the barrier for photoinduced electron transfer from the change in free energy for charge separation (ΔG_{cs}) and the reorganization energy (λ):[39]

$$\Delta G^{\ddagger}_{cs} = (\Delta G_{cs} + \lambda)^2/4\lambda \qquad (5)$$

The reorganization energy consists of internal (λ_i) and solvent (λ_s) contributions. The latter can be calculated in the Born−Hush approach via [22,28,40]

$$\lambda_s = \frac{e^2}{4\pi\epsilon_0}\left[\frac{1}{2}\left(\frac{1}{r^+} + \frac{1}{r^-}\right) - \frac{1}{R_{cc}}\right]\left(\frac{1}{n^2} - \frac{1}{\epsilon_s}\right) \qquad (6)$$

in which n is the refractive index of the solvent. For the internal reorganization energy, we estimate $\lambda_i = 0.3$ eV.[10c,22,28] The values for $\lambda = \lambda_i + \lambda_s$ obtained in this way are compiled in Table 4 for $n > 1$, together with the free-energy change (ΔG_{cs}) and barrier ($\Delta G^{\ddagger}_{cs}$) for intramolecular electron transfer in the OPV*n*-C_{60} dyads relative to the OPV*n*(S_1) and MP-C_{60}(S_1) excited states. Table 4 shows that the forward photoinduced charge separation in the OPV*n*-C_{60} dyads in ODCB originating from the MP-C_{60}(S_1) state is in the "normal" Marcus region ($\lambda > -\Delta G_{cs}$) and that the barrier for electron transfer in OPV*n*-C_{60} is less than ~0.1 eV for $n > 1$. Direct forward photoinduced charge separation originating from the OPV*n*(S_1) state would occur in the Marcus "inverted" region ($\lambda < -\Delta G_{cs}$), irrespective of the solvent or conjugation length of the OPV*n* donor (Table 4). The latter is a consequence of the higher energy of the singlet excited state. The estimates for $\Delta G^{\ddagger}_{cs}$ change only little when different values are used for λ_i; when λ_i is varied from 0.2 to 0.4 eV, $\Delta G^{\ddagger}_{cs}$ remains <0.1 eV for both OPV3-C_{60} and OPV4-C_{60} in ODCB.

The nonadiabatic charge separation rate constant is a function of the energy barrier $\Delta G^{\ddagger}_{cs}$, the reorganization energy, and the electronic coupling (V) between donor and acceptor in the excited state:[41]

$$k_{cs} = \left(\frac{4\pi^3}{h^2\lambda k_B T}\right)^{1/2} V^2 \exp\left[\frac{-\Delta G^{\ddagger}_{cs}}{k_B T}\right] \qquad (7)$$

Using the values for λ and for k_{cs} and $\Delta G^{\ddagger}_{cs}$ for the direct and indirect charge-transfer mechanisms as listed in Tables 3 and 4, it is possible to estimate the electronic coupling. For the indirect mechanism, that is, charge separation after singlet energy transfer, the values calculated for V using eq 7 and k_{cs}^{i} are $V^{i} = 30 \pm 3$ cm^{-1} for OPV3-C_{60} and OPV4-C_{60} in ODCB. For the direct mechanism, eq 7 indicates that V should be on the order of $V^{d} = 1300-2600$ cm^{-1} to explain the very high rate constants k_{cs}^{d}. Such a strong coupling would probably cause differences in the absorption spectrum of the OPV*n*-C_{60} dyads in comparison with the linear superposition of the spectra of OPV*n*'s and MP-C_{60}, which is not observed experimentally. Moreover, such coupling is much larger than the interaction expected between two chromophores separated by a bridge of three σ bonds.[28,42]

We conclude that the kinetic analysis supports the conclusion inferred from the residual OPV*n* fluorescence of the OPV*n*-C_{60} dyads in ODCB, that charge separation in these systems is preceded by energy transfer when the OPV*n* moiety is initially excited.

Conclusions

We have synthesized a novel series of oligo(*p*-phenylene vinylene)-fulleropyrrolidines OPV*n*-C_{60} and the corresponding model compounds OPV*n* and MP-C_{60}. Upon photoexcitation of the donor−acceptor dyads and OPV*n*/MP-C_{60} mixtures in solution, fast singlet energy transfer occurs. Depending on the conjugation length of the OPV*n* moiety/molecule and the relative permittivity of the medium, a charge-separated state may form in a subsequent reaction, in which an electron is transferred from the OPV*n* donor to the fullerene acceptor as the net result.

In an apolar solvent, toluene, the fluorescence and PIA spectra of the OPV*n*-C_{60} dyads provide clear evidence for efficient intramolecular photoinduced singlet energy transfer from the photoexcited OPV*n* moiety to the ground-state fullerene moiety, irrespective of the conjugation length. The fast energy transfer is followed by a nearly quantitative intersystem crossing to the fullerene triplet state. For mixtures of OPV*n* and MP-C_{60} in toluene, an intermolecular triplet energy transfer from the OPV*n*(T_1) state to the ground state of MP-C_{60} occurs, generating the corresponding MP-C_{60}(T_1) triplet state.

In the more polar solvent ODCB, photoexcitation of MP-C_{60} codissolved with OPV3 or OPV4 results in the formation of a charge-separated state, because of intermolecular electron transfer from ground-state OPV3 or OPV4 to the MP-C_{60}(T_1) state. For a cosolution of OPV2 and the fullerene derivative in ODCB, we do not observe photoinduced polaron absorptions.

Intramolecular charge-separated states are formed upon excitation of the OPV*n* moiety in solutions of OPV2-C_{60}, OPV3-C_{60}, or OPV4-C_{60} in ODCB. The quenching of the fullerene fluorescence in this more polar solvent indicates that the forward intramolecular electron transfer occurs within about 60 and 30 ps after the initial singlet energy transfer for OPV3-C_{60} and OPV4-C_{60}, respectively. Because the initial singlet energy transfer occurs within only 1 ps, these numbers also apply for the overall process from light absorption to charge separation. Charge separation is not observed for OPV1-C_{60} in ODCB. The observed discrimination between intra- and intermolecular energy and electron-transfer processes as a function of conjugation length and polarity of the solvent is in full agreement with the estimated free energies of the charge-separated state as derived from eq 2. The experimental result that the residual OPV*n* fluorescence of the OPV*n*-C_{60} dyads in ODCB is similar to that in toluene suggests that intramolecular photoinduced charge-separation occurs by an indirect mechanism, that is, after

singlet energy transfer from the OPV*n*(S_1) state to the MP-C_{60} moiety. This is supported by the strong electronic coupling (V^d), which would be necessary to explain the quenching of the fullerene emission by the direct mechanism. The conclusion of a two-step mechanism, however, contrasts with the experimental observation of subpicosecond electron transfer in conjugated polymer−fullerene blends.[2,3] Future experiments using ultrafast spectroscopic methods will be performed to investigate the temporal evolution of the photoexcitations in these dyads in more detail and to enhance our insight into the energy versus electron-transfer processes. Such studies will also elucidate the possible differences between electron transfer in these dyads in solution and in composite films of conjugated polymers and fullerenes.

In the solid phase (i.e., in thin films), long-lived charge-separated states are observed for OPV3-C_{60} and OPV4-C_{60} but not for OPV1-C_{60} and OPV2-C_{60}. The long lifetimes are attributed to intermolecular charge-separated states resulting from the migration of holes and/or electrons to other molecules in the films. Therefore, we conclude that the long lifetime of the charge-separated state is a material rather than a molecular property. From the longest dyad, OPV4-C_{60}, we have prepared photovoltaic devices. Although the device efficiency is not optimized, we find encouraging short-circuit currents ($I_{sc} = 235$ μA cm^{-2}) and open-circuit voltages ($V_{oc} = 650$ mV) under ~65 mW cm^{-2} white-light illumination. These findings indicate that the donor−acceptor dyads form a bicontinuous D−A network.[6,7] As an important clue for the future design of more efficient molecular bulkheterojunction materials, the action of the dyad device indicates clearly that concurrent electron and hole transport through a bicontinuous donor−acceptor network on even the finest molecular scale does not necessarily suffer from a massive charge recombination problem.

Experimental Section

General. UV/vis absorption spectra were recorded on a Perkin-Elmer Lambda 900 or a Perkin-Elmer Lambda 40 spectrophotometer. Low-temperature spectra were recorded using an Oxford Optistat continuous flow cryostat; during measurements the temperature was kept constant within 0.1 K. Spectra at different temperatures were not corrected for volume changes of the solvents. Fluorescence spectra were recorded on a Perkin-Elmer LS 50B spectrometer, using a 10 nm bandwidth and optical densities of the solutions of 0.1 at the excitation wavelength.

NMR spectra were recorded on a Varian Unity Plus spectrometer at frequencies of 500 and 125 MHz for ^{1}H and ^{13}C nuclei, respectively, on a Bruker AM-400 spectrometer at frequencies of 400 and 100 MHz for ^{1}H and ^{13}C nuclei, respectively, or on a Varian Gemini spectrometer at frequencies of 300 and 75 MHz for ^{1}H and ^{13}C nuclei, respectively. Tetramethylsilane (TMS) was used as an internal standard for ^{1}H NMR, and $CDCl_3$ or CS_2 was used as an internal standard for ^{13}C NMR. Infrared (FT-IR) spectra were recorded on a Perkin-Elmer 1605 FT-IR spectrophotometer or a Perkin-Elmer Spectrum One UATR FT-IR spectrophotometer. Elemental analyses were performed on a Perkin-Elmer 2400 series II CHN analyzer. Gas chromatography/mass spectrometry (GC−MS) analyses were performed on a Shimadzu GCMS-QP5000 equipped with a WCOT fused silica column (length = 15 m, i.d. = 0.25 mm). Matrix-assisted laser desorption ionization time-of-flight mass spectrometry (MALDI-TOF MS) was performed on a Perseptive DE PRO Voyager MALDI-TOF mass spectrometer using a dithranol matrix. Atmospheric pressure chemical ionization mass spectrometry (APCI-MS) was performed on a PE-Sciex API 300 MS/MS mass spectrometer with a mass range of 3000.

Cyclic Voltammetry. Cyclic voltammograms were recorded with 0.1 M tetrabutylammonium hexafluorophosphate (TBAH) as the supporting electrolyte using a Potentioscan Wenking POS73 potentiostat. The substrate concentration was typically 10^{-3} M. The working electrode was a platinum disk (0.2 cm^2), and the counter electrode was a platinum plate (0.5 cm^2). A saturated calomel electrode was used as reference electrode, calibrated against the Fc/Fc^+ couple (+0.470 V vs SCE).

Photoinduced Absorption. Photoinduced absorption (PIA) spectra were recorded between 0.25 and 3 eV by exciting with a mechanically modulated continuous wave Ar-ion laser pump beam and monitoring the resulting change in transmission (ΔT) after dispersion by a triple-grating monochromator, using Si, InGaAs, and InSb (cooled) detectors. The PIA spectra were recorded with the pump beam in an almost parallel direction to the probe beam. Oxygen-free solutions were studied at room temperature, whereas thin films were held at 80 ± 0.1 K, using an Oxford Optistat continuous flow cryostat. The changes in ΔT as a function of the pump beam intensity (I) were fitted to a power law equation $-\Delta T \propto I^p$. For values of p close to unity, we assumed monomolecular decay of the excited species; for $p \approx 0.5$ a bimolecular decay mechanism was supposed. Excited-state lifetimes were determined by fitting the changes in transmission as a function of the modulation frequency (ω) to the expressions for either monomolecular decay (eq 8) or bimolecular decay (eq 9).[25]

$$-\Delta T \propto \frac{Ig\tau_m}{\sqrt{1+\omega^2{\tau_m}^2}} \tag{8}$$

$$-\Delta T \propto \sqrt{Ig/\beta}\left(\frac{\alpha \tanh \alpha}{\alpha + \tanh \alpha}\right) \tag{9}$$

Here, τ_m is the lifetime for monomolecular decay and g is the efficiency of generation of the photoinduced species. The bimolecular decay constant β determines the intensity of the PIA signal via eq 9, where $\alpha = \pi/(\omega\tau_b)$ and $\tau_b = (gI\beta)^{-0.5}$, the bimolecular lifetime under steady-state conditions. It is important to note that the bimolecular lifetime, τ_b, depends on the experimental conditions such as concentration and pump beam intensity.

Photovoltaic Devices. The devices were prepared on poly(ethylene terephthalate) (PET) substrates covered with patterned indium−tin oxide (ITO) as the transparent electrode. First, the substrates were covered with polyethylenedioxythiophene polystyrenesulfonate (PEDOT−PSS, Baytron-P) to prevent shunting; subsequently a thin layer of the donor−acceptor dyad was deposited from a 2 wt % solution in toluene at 80 °C, using the doctor blade technique. Thin stripes of aluminum were deposited as counter electrodes by vacuum evaporation to form active areas of 6 mm^2.

Materials. C_{60} (99.5%) was purchased from Southern Chemical Group, LCC. All other reagents were purchased from Acros and Aldrich and used without further purification. For the PIA measurements, toluene was distilled over potassium/sodium and ODCB was dried over activated alumina and subsequently distilled at reduced pressure. For synthetic purposes, DMF was stored over BaO or 4.0 Å molecular sieves and THF and diethyl ether were distilled over potassium/sodium. For column chromatography, Merck silica gel 60 (particle size of 0.063−0.200 mm) or Merck aluminum oxide 90 (neutral; activity I, particle size of 0.063−0.200 mm) was used.

Abbreviations. AIBN, 2,2′-azobis(2-methylpropionitrile); *t*-BuO, *tert*-butoxide; DMF, *N*,*N*-dimethylformamide; NBS, *N*-bromosuccinimide; THF, tetrahydrofuran; R_f, thin-layer chromatography retention factor.

1,4-Bis[(*S*)-2-methylbutoxy]-2-methylbenzene (1). Methylhydroquinone (49.6 g, 0.40 mol), (*S*)-2-methylbutyl-*p*-toluenesulfonate (203.52 g, 0.84 mol), and tetrabutylammonium chloride (13.34 g, 0.048 mol) were added to a suspension of K_2CO_3 (332 g, 2.4 mol) in dry 2-butanone (400 mL) under an atmosphere of dry argon. The reaction mixture was stirred for 16 h at reflux temperature. After the mixture was cooled to room temperature, the suspension was filtered and the solvent was removed in vacuo. The resulting crude product was purified by column chromatography (silica gel, hexane/$CHCl_3$ 2:1, R_f = 0.8). Evaporation of the solvent yielded 99.3 g (94%) of **1** as a colorless oil: IR (UATR) 2961, 2918, 2876, 1501, 1465, 1215, 1045, 1011, 789 cm^{-1}; ^1H NMR ($CDCl_3$) δ 6.72 (dd, 1H), 6.68 (s, 1H), 6.63 (dd, 1H), 3.70 (m, 4H), 2.20 (s, 3H), 1.83 (m, 2H), 1.54 (m, 2H), 1.25 (m, 2H), 0.98 (m, 6H), 0.92 (m, 6H); ^{13}C NMR ($CDCl_3$) δ 152.95, 151.48, 127.97, 117.64, 111.85, 111.47, 73.40, 34.98, 34.81, 26.22, 26.16, 16.66, 16.52, 16.34, 11.36, 11.29; GC−MS (MW = 264.2) m/z = 264.2 $[M]^+$.

2,5-Bis[(*S*)-2-methylbutoxy]-4-methylbenzaldehyde (2). $POCl_3$ (96 mL, 1.05 mol) was added to a mixture of dry DMF (68 mL, 0.88 mol) and dry $CHCl_3$ (120 mL) under an atmosphere of dry argon. After the mixture was stirred for 1 h, **1** (63.36 g, 0.24 mol) was added and the reaction mixture was stirred for 48 h at reflux temperature. After the mixture was cooled to room temperature, the mixture was poured on ice−water (1500 mL), stirred for 1 h, and extracted with diethyl ether (500 mL); during the extraction NaCl was added to promote phase separation. The organic phase was washed with 1 M HCl (3 × 300 mL), water (3 × 300 mL), and a saturated $NaHCO_3$ solution (300 mL). After the organic phase was dried over $MgSO_4$ and the solvent was evaporated in vacuo, the crude product was purified by column chromatography (silica gel, hexane/$CHCl_3$ 2:1, R_f = 0.8). Recrystallization from methanol yielded 48.8 g (86%) of **2** as white crystals: IR (UATR) 2963, 2922, 2876, 2850, 1672, 1610, 1503, 1466, 1411, 1391, 1262, 1212, 1048, 1032, 1007, 877, 860, 760, 707 cm^{-1}; ^1H NMR ($CDCl_3$) δ 10.45 (s, 1H), 7.20 (s, 1H), 6.78 (s, 1H), 3.80 (m, 4H), 2.26 (s, 3H), 1.87 (m, 2H), 1.54 (m, 2H), 1.27 (m, 2H), 1.03 (t, 6H), 0.93 (m, 6H); ^{13}C NMR ($CDCl_3$) δ 189.20, 156.24, 136.74, 122.94, 122.94, 115.48, 108.03, 73.75, 73.12, 34.80, 34.74, 26.12, 26.06, 17.15, 16.56, 16.51, 11.25, 11.23; GC−MS (MW = 292.2) m/z = 292.3 $[M]^+$. Anal. Calcd for $C_{18}H_{28}O_3$: C, 73.93; H, 9.65. Found: C, 73.86; H, 9.54.

1-Bromo-2,5-bis[(*S*)-2-methylbutoxy]-4-bromomethylbenzene (3). NBS (53.4 g, 0.30 mol) and AIBN (15.0 g, 0.09 mol) were added to a solution of **1** (66.0 g, 0.25 mol) in dry CCl_4 (250 mL) under an atmosphere of dry argon. After the reaction mixture was stirred for 1 h under reflux, it was subsequently allowed to cool to room temperature and filtered. After evaporation of the solvent, hexane (100 mL) was added to the residue and the resulting suspension was filtered and evaporated to dryness. The remaining residue was dissolved in dry THF (250 mL); NBS (57.9 g, 0.325 mol) was added, and the reaction mixture was stirred at reflux temperature for 1 h. After evaporation of the solvent, hexane (100 mL) was added. The solution was filtered, and the solvent was removed in vacuo. Crystallization of the residue from ethanol yielded 55.8 g (53%) of **3** as a white crystalline solid: IR (UATR) 2961, 2922, 2875, 1495, 1462, 1388, 1296, 1220, 1205, 1044, 882, 862, 839, 745 cm^{-1}; ^1H NMR ($CDCl_3$) δ 7.03 (s, 1H), 6.86 (s, 1H), 4.49 (s, 2H), 3.81 (m, 2H), 3.74 (m, 2H), 1.88 (m, 2H), 1.57 (m, 2H), 1.21 (m, 2H), 1.04 (2d, 6H), 0.94 (t, 6H); ^{13}C NMR ($CDCl_3$) δ 151.18, 149.49, 125.90, 117.10, 115.71, 113.13, 74.78, 73.66, 34.80, 28.43, 26.09, 26.05, 16.65, 16.54, 11.33; GC−MS (MW = 420.0) m/z = 420.1 $[M]^+$. Anal. Calcd for $C_{17}H_{26}Br_2O_2$: C, 48.36; H, 6.21. Found: C, 48.59; H, 6.13.

Diethyl{2,5-bis[(*S*)-2-methylbutoxy]-4-bromo-benzyl}-phosphonate (4). Triethyl phosphite (15.6 g, 0.094 mol) and **3** (32.93 g, 0.078 mol) were stirred at 160 °C for 1.5 h while the liberated ethyl bromide was distilled off. The reaction mixture was cooled to 75 °C, and the excess triethyl phosphite was removed by distillation under reduced pressure to leave **4** (37.2 g, 100%) as a light yellow oil: ^1H NMR ($CDCl_3$) δ 7.02 (s, 1H), 6.96 (s, 1H), 4.02 (m, 4H), 3.74 (m, 4H), 3.18 (d, 2H), 1.86 (m, 2H), 1.56 (m, 2H), 1.30 (m, 2H), 1.25 (t, 6H), 1.02 (2d, 6H), 0.93 (t, 6H); ^{13}C NMR ($CDCl_3$) δ 150.81 (d), 149.18 (d), 119.99 (d), 116.52, 116.12 (d), 110.38 (d), 74.42, 73.66, 61.69 (d), 34.64, 34.60, 26.05 (d), 25.89, 25.84, 16.42, 16.31, 16.17, 16.11, 11.10.

(*E*)-4-{4-Methyl-2,5-bis[(*S*)-2-methylbutoxy]styryl}-2,5-bis[(*S*)-2-methylbutoxy]bromobenzene (5). A solution of aldehyde **2** (46.78 g, 0.16 mol) in dry DMF (300 mL) was added dropwise to a solution of **4** (76.72 g, 0.16 mol) and *t*-BuOK (20.6 g, 0.184 mol) in dry DMF (200 mL) under an atmosphere of dry argon. The resulting viscous reaction mixture was stirred for 8 h at room temperature and subsequently poured on crushed ice (1000 g). Aqueous HCl (5 M, 240 mL) was added, and the aqueous phase was extracted with $CHCl_3$ (3 × 300 mL). The combined organic layers were washed with 3 M HCl and dried over $MgSO_4$. The solvent was evaporated, and **5** (72.33 g, 73%) was obtained as a yellow solid after recrystallization from ethanol: IR (UATR) 2960, 2929, 2873, 1508, 1458, 1385, 1202, 1039, 970, 848 cm^{-1}; ^1H NMR ($CDCl_3$) δ 7.46 (d, 1H), 7.34 (d, 1H), 7.15 (s, 1H), 7.05 (2s, 2H), 6.71 (s, 1H), 3.80 (m, 8H), 2.22 (s, 3H), 1.89 (m, 4H), 1.60 (m, 4H), 1.31 (m, 4H), 1.04 (m, 12H), 0.96 (m, 12H); ^{13}C NMR ($CDCl_3$) δ 151.63, 150.80, 150.43, 149.93, 127.81, 127.49, 124.77, 123.73, 121.23, 117.99, 116.19, 111.03, 110.54, 108.39, 74.68, 74.56, 74.45, 73.35, 35.07, 34.95, 34.83, 26.31, 26.27, 26.24, 26.11, 16.78, 16.69, 16.58, 16.41, 11.45, 11.36, 11.34; APCI-MS (MW = 616.3) m/z = 617.5 $[M + H]^+$. Anal. Calcd for $C_{35}H_{53}BrO_4$: C, 68.06; H, 8.65. Found: C, 68.13; H, 8.59.

(*E*)-4-{4-Methyl-2,5-bis[(*S*)-2-methylbutoxy]styryl}-2,5-bis[(*S*)-2-methylbutoxy]benzaldehyde (6). Bromide **5** (37.24 g, 60.23 mmol) was dissolved in dry diethyl ether (400 mL). The solution was cooled to −10 °C, and 1.6 M *n*-butyllithium in hexane (60 mL) was added slowly. After the mixture was stirred for 5 min, the cooling bath was removed and dry DMF (21.3 mL) was added dropwise. The mixture was stirred for another hour at room temperature. After addition of 6 M HCl (100 mL), the organic layer was washed with water (2 × 250 mL), with a saturated $NaHCO_3$ solution (300 mL), and again with water (300 mL). The organic layer was dried over $MgSO_4$, and the solvent was evaporated. Recrystallization from methanol/diethyl ether (5:1) yielded 30.1 g (88%) of **6** as a yellow solid: IR (UATR) 2958, 2922, 2874, 1672, 1594, 1508, 1463, 1424, 1387, 1203, 1041, 966, 872, 727 cm^{-1}; ^1H NMR ($CDCl_3$) δ 10.45 (s, 1H), 7.61 (d, 1H), 7.42 (d, 1H), 7.31 (s, 1H), 7.21 (s, 1H), 7.07 (s, 1H), 6.72 (s, 1H), 3.81 (m, 8H), 2.23 (s, 3H), 1.91 (m, 4H), 1.61 (m, 4H), 1.31 (m, 4H), 1.05 (m, 12H), 0.95 (m, 12H); ^{13}C NMR ($CDCl_3$) δ 188.97, 156.42, 151.63, 150.78, 150.50, 135.42, 128.76, 126.79, 124.23, 123.79, 120.93, 116.09, 110.12, 109.46, 108.45, 74.44, 73.85, 73.63, 73.32, 35.05, 34.91, 34.69, 34.61, 26.22, 26.15, 16.77, 16.70, 16.60, 16.47, 11.44,

11.33, 11.28; GC−MS (MW = 566.4) m/z = 566.6 $[M]^+$. Anal. Calcd for $C_{36}H_{54}O_5$: C, 76.28; H, 9.60. Found: C, 76.23; H, 9.63.

(*E*,*E*)-4-{4-(4-Methyl-2,5-bis[(*S*)-2-methylbutoxy]styryl)-2,5-bis[(*S*)-2-methylbutoxy]styryl}-2,5-bis[(*S*)-2-methylbutoxy]-bromobenzene (7). According to the procedure for the synthesis of **5**, aldehyde **6** (3.40 g, 6.0 mmol, 20 mL of DMF) was added to a solution of **4** (2.88 g, 6.0 mmol) and *t*-BuOK (0.81 g, 7.2 mmol) in DMF (10 mL). Recrystallization from methanol yielded 4.28 g (80%) of **7** as a yellow-orange solid: IR (UATR) 2959, 2917, 2873, 1509, 1462, 1433, 1387, 1347, 1252, 1203, 1047, 964, 851 cm^{-1}; ^1H NMR ($CDCl_3$) δ 7.54−7.38 (4d, 4H), 7.19 (s, 1H), 7.17 (s, 1H), 7.15 (s, 1H), 7.10 (s, 1H), 7.08 (s, 1H), 6.72 (s, 1H), 3.82 (m, 12H), 2.23 (s, 3H), 1.92 (m, 6H), 1.63 (m, 6H), 1.22 (m, 6H), 1.06 (m, 18H), 0.97 (m, 18H); ^{13}C NMR ($CDCl_3$) δ 151.68, 151.13, 150.93, 150.46, 149.97, 127.92, 127.62, 127.38, 126.69, 125.15, 123.49, 123.19, 122.03, 121.63, 118.01, 116.28, 111.32, 110.65, 110.21, 109.86, 108.37, 74.71, 74.65, 74.47, 74.30, 74.17, 73.37, 35.11, 35.05, 34.96, 34.64, 26.36, 26.29, 26.26, 26.12, 16.80, 16.73, 16.70, 16.59, 16.40, 11.45, 11.36, 11.33; APCI-MS (MW = 890.5) m/z = 891.8 $[M + H]^+$. Anal. Calcd for $C_{53}H_{79}BrO_6$: C, 71.36; H, 8.93. Found: C, 71.12; H, 9.01.

(*E*,*E*)-4-{4-(4-Methyl-2,5-bis[(*S*)-2-methylbutoxy]styryl)-2,5-bis[(*S*)-2-methylbutoxy]styryl}-2,5-bis[(*S*)-2-methylbutoxy]-benzaldehyde (8). According to the procedure for the synthesis of **6**, compound **7** (5.0 g, 5.6 mmol, 75 mL diethyl ether) was treated subsequently with *n*-butyllithium (1.6 M in hexane, 5.6 mL) and dry DMF (2.5 mL). Recrystallization from hexane yielded 4.08 g (86%) of **8** as an orange solid: IR (UATR) 2958, 2917, 2874, 1675, 1508, 1463, 1422, 1388, 1347, 1261, 1201, 1120, 1043, 1008, 965, 849, 725 cm^{-1}; ^1H NMR ($CDCl_3$) δ 10.47 (s, 1H), 7.64 (d, 1H), 7.53 (d, 1H), 7.52 (d, 1H), 7.46 (d, 1H), 7.32 (s, 1H), 7.24 (s, 1H), 7.20 (s, 1H), 7.17 (s, 1H), 7.10 (s, 1H), 6.72 (s, 1H), 3.83 (m, 12H), 2.24 (s, 3H), 1.93 (m, 6H), 1.62 (m, 6H), 1.33 (m, 6H), 1.07 (m, 18H), 0.96 (m, 18H); ^{13}C NMR ($CDCl_3$) δ 188.94, 156.36, 151.61, 151.39, 150.84, 150.54, 150.44, 135.19, 128.67, 127.74, 126.45, 126.00, 124.91, 123.64, 123.56, 121.61, 121.40, 116.17, 110.23, 110.06, 109.67, 109.48, 108.24, 74.53, 74.19, 74.02, 73.82, 73.58, 73.28, 35.05, 34.98, 34.90, 34.84, 34.78, 26.30, 26.21, 26.13, 16.76, 16.70, 16.66, 16.58, 16.39, 11.44, 11.34, 11.28; APCI-MS (MW = 840.6) m/z = 842.0 $[M + H]^+$.

(*E*,*E*,*E*)-4-[4-{4-(4-Methyl-2,5-bis[(*S*)-2-methylbutoxy]styryl)-2,5-bis[(*S*)-2-methylbutoxy]styryl}-2,5-bis[(*S*)-2-methylbutoxy]-styryl]-2,5-bis[(*S*)-2-methylbutoxy]bromobenzene (9). According to the procedure for the synthesis of **5**, aldehyde **8** (1.35 g, 1.6 mmol) in DMF (25 mL, 40 °C) was added to a solution of **4** (0.79 g, 1.65 mmol) and *t*-BuOK (0.24 g, 2.15 mmol) in dry DMF (5 mL). Precipitation from $CHCl_3$ into methanol and recrystallization from 2-propanol afforded 1.30 g (70%) of **9** as an orange solid: IR (UATR) 2958, 2918, 2873, 2859, 1507, 1463, 1420, 1386, 1347, 1251, 1201, 1045, 965, 852 cm^{-1}; ^1H NMR ($CDCl_3$) δ 7.56−7.36 (6d, 6H), 7.19 (3s, 3H), 7.17 (2s, 2H), 7.11 (s, 1H), 7.08 (s, 1H), 6.73 (s, 1H), 3.83 (m, 16H), 2.23 (s, 3H), 1.94 (m, 8H), 1.64 (m, 8H), 1.34 (m, 8H), 1.08 (m, 24H), 0.98 (m, 24H); ^{13}C NMR ($CDCl_3$) δ 151.63, 151.08, 151.01, 150.89, 150.40, 149.92, 127.70, 127.67, 127.54, 127.27, 127.00, 126.87, 125.14, 123.39, 123.01, 122.85, 122.38, 122.10, 121.63, 117.94, 116.25, 111.33, 110.56, 110.07, 110.03, 109.86, 109.84, 108.27, 74.62, 74.41, 74.18, 74.13, 73.31, 35.08, 35.02, 34.93, 34.81, 26.35, 26.27, 26.24, 26.10, 16.79, 16.73, 16.69, 16.58, 16.40, 11.46, 11.36, 11.34; APCI-MS (MW = 1164.7) m/z = 1165.8 $[M + H]^+$. Anal. Calcd for $C_{71}H_{105}BrO_8$: C, 73.11; H, 9.07. Found: C, 73.40; H, 9.16.

(*E*,*E*,*E*)-4-[4-{4-(4-Methyl-2,5-bis[(*S*)-2-methylbutoxy]styryl)-2,5-bis[(*S*)-2-methylbutoxy]styryl}-2,5-bis[(*S*)-2-methylbutoxy]-styryl]-2,5-bis[(*S*)-2-methylbutoxy]benzaldehyde (10). *n*-Butyllithium (1.6 M, 1.5 mL) was added slowly at −10 °C to a stirred solution of compound **9** (1.17 g, 1.0 mmol) in a mixture of dry THF (20 mL) and dry diethyl ether (30 mL) under an atmosphere of dry argon. After 30 min, the cooling bath was removed, dry DMF (1 mL) was added, and the mixture was stirred for 1 h at room temperature. After addition of 6 M HCl (4 mL), the aqueous layer was extracted with CH_2Cl_2. The organic fractions were collected, and the solvent was evaporated. The residue was dissolved in $CHCl_3$ and then washed with water and dried over Na_2SO_4. The solvent was evaporated, and the residue was precipitated from $CHCl_3$ into methanol and further purified by column chromatography (aluminum oxide, gradient; hexane/diethyl ether 3:1 → diethyl ether) to yield 0.30 g (27%) of **10**: IR (UATR) 2958, 2921, 2873, 2858, 1678, 1593, 1507, 1464, 1420, 1386, 1346, 1251, 1201, 1044, 966, 852, 725 cm^{-1}; ^1H NMR ($CDCl_3$) δ 10.45 (s, 1H), 7.66 (d, 1H), 7.60−7.42 (5d, 5H), 7.34 (s, 1H), 7.25 (s, 1H), 7.21 (s, 1H), 7.20 (s, 1H), 7.19 (s, 1H), 7.18 (s, 1H), 7.11 (s, 1H), 6.74 (s, 1H), 3.86 (m, 16H), 2.23 (s, 3H), 1.94 (m, 8H), 1.62 (m, 8H), 1.34 (m, 8H), 1.06 (m, 24H), 0.97 (m, 24H); ^{13}C NMR ($CDCl_3$) δ 188.96, 156.44, 151.72, 151.49, 151.24, 151.07, 151.1, 150.68, 150.52, 135.27, 128.65, 127.96, 127.64, 126.96, 126.53, 126.36, 125.23, 124.04, 123.41, 123.21, 122.33, 121.86, 121.70, 116.33, 110.36, 110.26, 110.20, 109.95, 109.70, 108.45, 74.70, 74.33, 74.25, 74.17, 73.95, 73.75, 73.43, 35.14, 35.06, 34.99, 34.92, 34.87, 26.39, 26.28, 26.20, 16.81, 16.75, 16.70, 16.63, 16.37, 11.45, 11.35, 11.29; APCI-MS (MW = 1114.8) m/z = 1116.0 $[M + H]^+$.

***N*-Methyl-2-{4-methyl-2,5-bis[(*S*)-2-methylbutoxy]phenyl}-3,4-fulleropyrrolidine (OPV1-C_{60}).** *N*-Methylglycine (287 mg, 3.0 mmol) and **2** (292 mg, 1.0 mmol) were added to a solution of C_{60} (0.72 g, 1.0 mmol) in chlorobenzene (200 mL) under an atmosphere of dry argon. The reaction mixture was stirred at reflux temperature for 16 h in the dark. The solvent was evaporated, and the residue was purified by column chromatography (silica gel). Elution with CS_2 afforded unreacted C_{60}, and further elution with cyclohexane/toluene (3:1) afforded the desired product fraction (R_f = 0.3). The product fraction was concentrated in vacuo to a volume of ∼10 mL and precipitated by addition of methanol. The precipitate was washed three times with methanol to afford 452 mg (44%) of OPV1-C_{60} (mixture of two diastereomers) as a brown powder: IR (KBr) 2956, 2910, 2870, 2778, 1503, 1462, 1200, 1032, 770 cm^{-1}; ^1H NMR (CS_2, D_2O insert) δ 7.49 (s, 0.5H), 7.48 (s, 0.5H), 6.78 (s, 1H), 5.59 (s, 1H), 5.06 (d, 1H), 4.41 (d, 1H), 4.02−3.66 (m, 4H), 2.92 (s, 1.5H), 2.91 (s, 1.5H), 2.32 (s, 3H), 1.98 (m, 1H), 1.88−1.55 (m, 3H), 1.51−1.27 (m, 2H), 1.24−1.00 (m, 12H); ^{13}C NMR (CS_2, D_2O insert) δ 156.55, 156.54, 155.00, 154.94, 154.34, 154.31, 153.61, 153.60, 151.28, 151.19, 150.97, 147.02, 147.01, 146.61, 146.59, 146.51, 146.18, 146.17, 146.03, 145.99, 145.96, 145.89, 145.84, 145.81, 145.71, 145.70, 144.46, 144.35, 144.26, 144.12, 142.88, 142.81, 142.46, 142.43, 142.39, 142.36, 142.09, 142.08, 142.06, 142.03, 141.95, 141.89, 141.77, 141.54, 141.53, 141.51, 141.43, 141.42, 140.01, 139.93, 139.54, 139.40, 136.36, 136.35, 135.95, 135.85, 135.83, 134.41, 134.36, 127.20, 127.18, 122.41, 122.34, 114.53, 114.44, 112.42, 112.30, 76.47, 75.37, 75.34, 73.13, 73.08, 73.04, 72.98, 69.65, 68.93, 39.97, 35.21, 35.19, 35.13, 26.75, 26.50, 17.00, 16.96, 16.95, 16.80, 16.76, 12.03, 11.99, 11.97, 11.93; MALDI-TOF MS (MW = 1039.3)

$m/z = 1039.6$ $[M + H]^+$. Anal. Calcd for $C_{80}H_{33}NO_2$: C, 92.38; H, 3.20; N, 1.35. Found: C, 92.15; H, 3.15; N, 1.33.

***N*-Methyl-2-{4-(4-methyl-2,5-bis[(*S*)-2-methylbutoxy]styryl)-2,5-bis[(*S*)-2-methylbutoxy]phenyl}-3,4-fulleropyrrolidine (OPV2-C_{60}).** According to the synthetic procedure for OPV1-C_{60}, C_{60} (720 mg, 1.0 mmol) was mixed with *N*-methylglycine (287 mg, 3.0 mmol) and **6** (566 mg, 1.0 mmol) in chlorobenzene (200 mL). Chromatography (silica gel, CS_2 then cyclohexane/toluene 2:1, $R_f = 0.3$), precipitation, and washing yielded 614 mg (47%) of OPV2-C_{60} (mixture of two diastereomers) as a brown powder: IR (KBr) 2956, 2944, 2871, 2776, 1504, 1461, 1412, 1195, 1040, 968, 852, 768 cm^{-1}; ^1H NMR (CS_2, D_2O insert) δ 7.59 (s, 0.5H), 7.58 (s, 0.5H), 7.42 (d, 1H), 7.24 (d, 1H), 7.17 (s, 1H), 6.99 (s, 1H), 6.69 (s, 1H), 5.63 (s, 1H), 5.07 (d, 1H), 4.43 (d, 1H), 4.08−3.73 (m, 8H), 2.95 (s, 3H), 2.31 (s, 3H), 2.02 (m, 3H), 1.93−1.56 (m, 5H), 1.54−1.28 (m, 4H), 1.27−1.02 (m, 24H); ^{13}C NMR (CS_2, D_2O insert) δ 156.48, 156.47, 154.90, 154.84, 154.18, 154.15, 153.51, 151.56, 151.19, 150.59, 150.50, 150.11, 147.03, 147.01, 146.57, 146.55, 146.49, 146.12, 146.11, 146.04, 145.98, 145.96, 145.89, 145.85, 145.81, 145.71, 145.47, 145.43, 145.34, 145.23, 145.15, 145.03, 145.01, 144.99, 144.97, 144.93, 144.87, 144.47, 144.33, 144.27, 144.11, 142.87, 142.81, 142.46, 142.43, 142.38, 142.36, 142.08, 142.06, 142.03, 141.96, 141.95, 141.92, 141.88, 141.76, 141.59, 141.52, 141.49, 141.48, 141.47, 140.02, 139.94, 139.64, 139.47, 139.46, 136.33, 135.94, 135.86, 135.84, 134.43, 134.38, 127.85, 128.83, 127.02, 124.70, 124.44, 124.38, 123.63, 123.61, 121.28, 115.64, 114.25, 114.13, 108.61, 108.51, 108.00, 76.50, 75.39, 75.36, 73.95, 73.89, 73.82, 72.90, 72.85, 72.73, 69.67, 68.95, 39.96, 35.34, 35.25, 35.17, 35.16, 35.14, 26.82, 26.79, 26.75, 26.46, 17.02, 16.99, 16.97, 16.76, 16.69, 16.68, 12.01, 11.99, 11.97, 11.94, 11.85; MALDI-TOF MS (MW = 1313.4) $m/z = 1314.2$ $[M + H]^+$. Anal. Calcd for $C_{98}H_{59}NO_4$: C, 89.54; H, 4.52; N, 1.07. Found: C, 89.35; H, 4.45; N, 0.99.

***N*-Methyl-2-{4-[4-(4-methyl-2,5-bis[(*S*)-2-methylbutoxy]-styryl)-2,5-bis[(*S*)-2-methylbutoxy]styryl]-2,5-bis[(*S*)-2-methylbutoxy]phenyl}-3,4-fulleropyrrolidine (OPV3-C_{60}).** Analogous to the synthesis of OPV1-C_{60}, C_{60} (720 mg, 1.0 mmol) was mixed with *N*-methylglycine (287 mg, 3.0 mmol) and **8** (841 mg, 1.0 mmol) in chlorobenzene (200 mL). After chromatography (silica gel, CS_2 then cyclohexane/toluene 3:2, $R_f = 0.25$), precipitation, and washing, 762 mg (48%) of OPV3-C_{60} (mixture of two diastereomers) was obtained as a brown powder: IR (KBr) 2957, 2912, 2871, 1504, 1461, 1414, 1381, 1335, 1245, 1197, 1041, 968, 855, 769 cm^{-1}; ^1H NMR (CS_2, D_2O insert) δ 7.62 (s, 0.5H), 7.61 (s, 0.5H), 7.48 (d, 1H), 7.43 (2d, 1H), 7.42 (d, 1H), 7.36 (d, 1H), 7.21 (s, 1H), 7.11 (s, 1H), 7.10 (s, 1H), 7.02 (s, 1H), 6.71 (s, 1H), 5.65 (s, 1H), 5.09 (d, 1H), 4.45 (d, 1H), 4.11−3.77 (m, 12H), 2.97 (2s, 3H), 2.34 (s, 3H), 2.06 (m, 5H), 1.96−1.59 (m, 7H), 1.58−1.33 (m, 6H), 1.32−1.00 (m, 36H); ^{13}C NMR (CS_2, D_2O insert) δ 156.47, 156.46, 154.88, 154.82, 154.16, 154.13, 153.51, 153.50, 151.56, 151.21, 150.71, 150.69, 150.60, 150.52, 150.09, 147.03, 147.02, 146.56, 146.54, 146.49, 146.11, 146.10, 146.04, 145.99, 145.97, 145.90, 145.86, 145.82, 145.72, 145.47, 145.43, 145.34, 145.23, 145.16, 145.04, 145.02, 145.00, 144.98, 144.94, 144.88, 144.48, 144.33, 144.28, 144.12, 142.88, 142.82, 142.47, 142.44, 142.39, 142.37, 142.07, 142.04, 141.97, 141.95, 141.93, 141.89, 141.76, 141.60, 141.52, 141.51, 141.49, 141.48, 140.03, 139.95, 139.66, 139.48, 136.33, 136.32, 135.95, 135.86, 135.84, 134.43, 134.39, 127.72, 127.70, 127.53, 126.86, 126.44, 124.94, 124.68, 124.63, 123.33, 123.31, 122.94, 121.99, 121.39, 115.68, 114.23, 114.10, 109.62, 109.32, 108.65, 108.55, 107.87, 76.51, 75.40, 75.36, 73.94, 73.87, 73.57, 73.48, 72.91, 72.86, 72.71, 69.67, 68.95, 39.98, 39.97, 35.36, 35.30, 35.27, 35.23, 35.18, 35.16, 26.80, 26.76, 26.46, 17.04, 17.01, 16.99, 16.96, 16.76, 16.70, 16.69, 12.01, 11.99, 11.97, 11.93, 11.90, 11.85; MALDI-TOF MS (MW = 1587.6) $m/z = 1588.7$ $[M + H]^+$. Anal. Calcd for $C_{116}H_{85}NO_6$: C, 87.69; H, 5.39; N, 0.88. Found: C, 87.70; H, 5.30; N, 0.84.

***N*-Methyl-2-(4-{4-[4-(4-methyl-2,5-bis[(*S*)-2-methylbutoxy]-styryl)-2,5-bis[(*S*)-2-methylbutoxy]styryl]-2,5-bis[(*S*)-2-methylbutoxy]styryl}-2,5-bis[(*S*)-2-methylbutoxy]phenyl)-3,4-fulleropyrrolidine (OPV4-C_{60}).** Similar to the procedure for the synthesis of OPV1-C_{60}, C_{60} (216 mg, 0.3 mmol) was mixed with *N*-methylglycine (80 mg, 0.9 mmol) and **8** (335 mg, 0.3 mmol) in chlorobenzene (70 mL). After column chromatography (silica gel, CS_2 then cyclohexane/toluene 1:1, $R_f = 0.25$), a fluorescent contamination was still present. Further purification by column chromatography (silica gel, pentane/CH_2Cl_2 3:2, $R_f = 0.12$), precipitation, and washing afforded 224 mg (40%) of OPV4-C_{60} (mixture of two diastereomers) as a yellow-brown powder: IR (KBr) 2958, 2912, 2872, 1504, 1462, 1419, 1384, 1254, 1200, 1043, 968, 853, 770 cm^{-1}; ^1H NMR (CS_2, D_2O insert) δ 7.62 (s, 0.5H), 7.61 (s, 0.5H), 7.49 (d, 1H), 7.48−7.43 (3d, 3H), 7.73 (d, 1H), 7.38 (d, 1H), 7.21 (s, 1H), 7.13 (s, 1H), 7.12 (s, 1H), 7.11 (2s, 2H), 7.03 (s, 1H), 6.72 (s, 1H), 5.66 (s, 1H), 5.10 (d, 1H), 4.46 (d, 1H), 4.11−3.77 (m, 16H), 2.98 (s, 1.5H), 2.97 (s, 1.5H), 2.34 (s, 3H), 2.07 (m, 7H), 1.93−1.60 (m, 9H), 1.59−1.31 (m, 8H), 1.30−1.02 (m, 48H); ^{13}C NMR (CS_2, D_2O insert) δ 156.47, 156.45, 154.88, 154.81, 154.15, 154.12, 153.51, 151.56, 151.22, 150.72, 150.71, 150.63, 150.56, 150.09, 147.03, 147.02, 146.56, 146.54, 146.49, 146.11, 146.04, 145.99, 145.97, 145.90, 145.86, 145.82, 145.72, 145.47, 145.43, 145.34, 145.23, 145.16, 145.04, 145.02, 145.00, 144.98, 144.94, 144.88, 144.48, 144.33, 144.28, 144.12, 142.82, 142.47, 142.44, 142.39, 142.37, 142.07, 142.03, 141.97, 141.95, 141.93, 141.89, 141.76, 141.60, 141.52, 141.51, 140.03, 139.95, 139.66, 139.48, 136.33, 135.95, 135.86, 135.84, 134.44, 134.39, 127.69, 127.67, 127.40, 127.38, 126.82, 126.71, 126.67, 125.00, 124.74, 124.68, 123.30, 123.28, 122.83, 122.61, 122.12, 121.45, 115.70, 114.23, 114.11, 109.58, 109.45, 109.35, 108.66, 108.56, 107.87, 76.51, 75.40, 75.37, 73.93, 73.89, 73.57, 73.51, 72.92, 72.90, 72.88, 72.72, 69.68, 68.95, 39.97, 35.37, 35.29, 35.27, 35.23, 35.18, 35.16, 26.81, 26.76, 26.46, 17.03, 16.99, 16.96, 16.76, 16.70, 12.01, 11.99, 11.97, 11.94, 11.90, 11.85; MALDI-TOF MS (MW = 1861.8) $m/z = 1861.4$ $[M + H]^+$. Anal. Calcd for $C_{134}H_{111}NO_8$: C, 86.38; H, 6.00; N, 0.75. Found: C, 86.30; H, 5.91; N, 0.78.

(*E*)-1,2-Bis{4-methyl-2,5-bis[(*S*)-2-methylbutoxy]phenyl}-ethane (OPV2). Zinc dust (1.18 g, 18.0 mmol) was suspended in dry THF (50 mL) under an atmosphere of dry argon. $TiCl_4$ (1.0 mL, 9.0 mmol) was added dropwise at −10 °C, and then the mixture was stirred for 1 h at reflux temperature. Aldehyde **2** (0.88 g, 3.0 mmol) in dry THF (5 mL) was added, and the solution was stirred for another 16 h at reflux temperature. After the solution was cooled to room temperature, 10% aqueous K_2CO_3 (75 mL) was added under vigorous stirring. The stirring was continued for 30 min, and the dark blue solid that formed was filtered. The solid was thoroughly washed with $CHCl_3$. The chloroform extracts were combined, and the solvent was evaporated. The residue was dissolved in hexane and filtered, and the solvent was removed in vacuo. Recrystallization from 2-propanol/ethanol (9:1) yielded 0.26 g (31%) of OPV2: mp 73.5 °C; IR (KBr) 2960, 2929, 2874, 1512, 1464, 1411, 1391, 1249, 1208, 1047, 972, 855, 708 cm^{-1}; ^1H NMR ($CDCl_3$) δ 7.41 (s, 2H), 7.08 (s, 2H), 6.70 (s, 2H), 3.87−3.70 (m, 8H), 2.31 (s, 6H), 1.89 (m, 4H), 1.60 (m, 4H), 1.21 (m, 4H), 1.05

(m, 12H), 0.95 (m, 12H); ^{13}C NMR ($CDCl_3$) δ 151.66, 150.25, 127.16, 125.27, 121.98, 116.35, 108.22, 74.70, 73.31, 35.11, 34.95, 26.31, 26.24, 16.77, 16.69, 16.36, 11.47, 11.37; GC−MS (MW = 552.4) m/z = 552.6 $[M]^+$. Anal. Calcd for $C_{36}H_{56}O_4$: C, 78.21; H, 10.21. Found: C, 77.92; H, 10.72.

(*E*,*E*,*E*)-1,2-Bis(4-{4-methyl-2,5-bis[(*S*)-2-methylbutoxy]-styryl}-2,5-bis[(*S*)-2-methylbutoxy]phenyl)ethene (OPV4). Analogous to the synthesis of OPV2, aldehyde **6** (1.70 g, 3.0 mmol) in dry DMF (20 mL) was mixed with a reductive mixture of zinc (1.18 g, 18.0 mmol) and $TiCl_4$ (1.0 mL, 9.0 mmol) in dry THF (50 mL). Recrystallization from hexane yielded 0.69 g (41%) of OPV4: mp 204 °C; IR (KBr) 2960, 2917, 2874, 1509, 1566, 1421, 1389, 1350, 1252, 1204, 1047, 968, 853, 711 cm^{-1}; ^{1}H NMR ($CDCl_3$) δ 7.63 (s, 2H), 7.51 (d, 2H), 7.46 (d, 2H), 7.20 (2s, 4H), 7.11 (s, 2H), 6.73 (s, 2H), 3.96−3.70 (m, 16H), 2.23 (s, 6H), 1.93 (m, 8H), 1.64 (m, 8H), 1.35 (m, 8H), 1.16−0.90 (m, 48H); ^{13}C NMR ($CDCl_3$) δ 151.63, 151.07, 150.93, 150.40, 127.55, 127.49, 127.14, 125.17, 122.93, 122.51, 121.65, 116.25, 110.00, 109.85, 108.25, 74.62, 74.22, 73.30, 35.08, 35.04, 35.93, 26.36, 26.32, 26.24, 16.79, 16.69, 16.39, 11.47, 11.36. Anal. Calcd for $C_{72}H_{108}O_8$: C, 78.50; H, 9.88. Found: C, 78.61; H, 10.27.

1,4-Bis[(*S*)-2-methylbutoxy]benzene (11). Ground KOH (16.00 g, 285 mmol) was added to EtOH (250 mL), and the mixture was stirred for 20 min. Upon addition of hydroquinone (12.10 g, 110 mmol), the solution turned dark brown. After the solution was stirred for another 30 min, the reaction mixture was heated to reflux temperature and after 15 min (*S*)-2-methylbutyl-*p*-toluenesulfonate (58.64 g, 242 mmol) was added dropwise. The resulting suspension was stirred for another 16 h, cooled to room temperature, and filtered. The solvent was evaporated, and purification by column chromatography (silica gel, hexane/CH_2Cl_2 3:2, R_f = 0.55) yielded 20.76 g (75%) of **11** as a white solid: IR (UATR) 2961, 2914, 2876, 1506, 1466, 1389, 1225, 1042, 822, 780 cm^{-1}; ^{1}H NMR ($CDCl_3$) δ 6.80 (s, 4H), 3.80−3.60 (m, 4H), 1.82 (m, 2H), 1.55 (m, 2H), 1.22 (m, 2H), 1.03−0.86 (m, 12H); ^{13}C NMR ($CDCl_3$) δ 153.34, 115.34, 73.54, 34.77, 26.13, 16.51, 11.29; GC−MS (MW = 250.2) m/z = 250.2 $[M]^+$.

1,4-Bischloromethyl-2,5-bis[(*S*)-2-methylbutoxy]benzene (12). A solution of **11** (10.04 g, 40.1 mmol) in 1,4-dioxane (60 mL) was cooled to 0 °C, and 37% aqueous HCl (35 mL) was added. HCl gas was bubbled through the solution while 36% aqueous formaldehyde (20 mL) was added dropwise. Under continuous purging with HCl gas, the reaction mixture was stirred at room temperature for 1.5 h and cooled to 0 °C. Another portion of 36% aqueous formaldehyde (15 mL) was added dropwise; the mixture was subsequently stirred at room temperature for 1 h and cooled to 0 °C, and aqueous formaldehyde (10 mL) was added once more. The reaction mixture was heated to 60 °C and stirred for 16 h; after 2 h the purging with HCl gas was stopped. The reaction mixture was concentrated to about 15 mL; methanol (150 mL) was added, and the suspension was filtered. The solid was recrystallized from hexane to afford 10.15 g (73%) of **12** as transparent crystals: IR (UATR) 2959, 2923, 2876, 1515, 1465, 1442, 1416, 1395, 1313, 1226, 1137, 1039, 918, 872, 739, 706 cm^{-1}; ^{1}H NMR ($CDCl_3$) δ 6.89 (s, 2H), 4.63 (s, 4H), 3.90−3.70 (m, 4H), 1.88 (m, 2H), 1.56 (m, 2H), 1.30 (m, 2H), 1.03 (d, 6H), 0.95 (t, 6H); ^{13}C NMR ($CDCl_3$) δ 150.35, 126.68, 114.06, 73.66, 41.40, 34.88, 26.12, 16.64, 11.36; GC−MS (MW = 346.1) m/z = 346.2 $[M]^+$.

Tetraethyl{2,5-bis[(*S*)-2-methylbutoxy]-1,4-phenylenebis-(methylene)]bisphosphonate (13). Triethyl phosphite (3.00 g, 18.0 mmol) and **12** (2.50 g, 7.2 mol) were stirred at 160 °C for 4 h, and the liberated ethyl chloride was distilled off. Column chromatography (silica gel, ethyl acetate) afforded pure **13** (2.50 g, 63%) as a white solid: IR (UATR) 2966, 2930, 2878, 1514, 1463, 1418, 1390, 1240, 1218, 1030, 954, 896, 830, 777, 722 cm^{-1}; ^{1}H NMR ($CDCl_3$) δ 6.85 (d, 2H), 3.94 (m, 8H), 3.74−3.60 (m, 4H), 3.15 (d, 4H), 1.77 (m, 2H), 1.49 (m, 2H), 1.22 (m, 2H), 1.15 (dt, 12H), 0.95 (d, 6H), 0.87 (t, 6H); ^{13}C NMR ($CDCl_3$) δ 150.55 (d), 119.52 (d), 114.88 (d), 73.83, 61.96 (d), 35.13, 27.06, 26.33, 25.67 (d), 16.83, 16.53, 16.47, 11.50; GC−MS (MW = 550.3) m/z = 550.4 $[M]^+$.

(*E*,*E*)-1,4-Bis{4-methyl-2,5-bis[(*S*)-2-methylbutoxy]styryl}-2,5-bis[(*S*)-2-methylbutoxy]benzene (OPV3). Bisphosphonate **13** (0.28 g, 0.5 mmol) was dissolved in dry DMF (5 mL) under an argon atmosphere, and *t*-BuOK (0.17 g, 1.5 mmol) was added. After 15 min, aldehyde **2** (0.29 g, 1.0 mmol), dissolved in dry DMF (10 mL), was added dropwise, and the reaction mixture was stirred for 4 h. The solution was poured on crushed ice, and 6 M HCl (6 mL) was added. The aqueous phase was extracted with $CHCl_3$ (2 × 20 mL), and the combined organic layers were subsequently washed with 3 M HCl and water. The organic layer was dried over Na_2SO_4; the solvent was removed in vacuo, and the residue was purified by column chromatography (aluminum oxide, hexane/diethyl ether 2:1). Evaporation of the solvent afforded 120 mg (29%) of OPV3 as a yellow solid: mp 138 °C; IR (KBr) 2960, 2916, 2874, 1511, 1468, 1422, 1390, 1347, 1252, 1206, 1049, 972, 854, 711 cm^{-1}; ^{1}H NMR ($CDCl_3$) δ 7.49 (d, 2H), 7.44 (d, 2H), 7.17 (s, 2H), 7.09 (s, 2H), 6.71 (s, 2H), 3.94−3.68 (m, 12H), 2.23 (s, 6H), 1.90 (m, 6H), 1.62 (m, 6H), 1.33 (m, 6H), 1.06 (m, 18H), 0.96 (m, 18H); ^{13}C NMR ($CDCl_3$) δ 151.65, 150.95, 150.39, 127.46, 127.32, 125.23, 122.82, 121.73, 116.28, 109.94, 108.29, 74.66, 74.24, 73.33, 35.10, 35.05, 34.95, 26.36, 26.33, 26.24, 16.79, 16.70, 16.40, 11.47, 11.38; APCI-MS (MW = 826.6) m/z = 828 $[M + H]^+$. Anal. Calcd for $C_{54}H_{82}O_6$: C, 78.40; H, 9.99. Found: C, 78.35; H, 10.40.

Acknowledgment. We thank Mr. J. L. J. van Dongen for recording the mass spectra, Ms. J. J. Apperloo for recording the electrochemical data, and Dr. R. P. Sijbesma and Dr. L. Sanchez for assistance in computational chemistry. These investigations were supported by the Council for Chemical Sciences (CW) with financial aid from The Netherlands Technology Foundation (STW, 349-3562). Further support was obtained from The Netherlands Organization for Energy and Environment (NOVEM) in the NOZ-PV program (146.120-008.1 and 146.120.008.3), the Dutch Ministry of Economic Affairs, the Ministry of Education, Culture and Science, the Ministry of Housing, Spatial Planning and the Environment through the E.E.T. program (EETK97115), the Council for Chemical Sciences of The Netherlands Organization for Scientific Research (CW-NWO), and the Eindhoven University of Technology in the PIONIER program (98400).

References and Notes

(1) Sariciftci, N. S.; Smilowitz, L.; Heeger, A. J.; Wudl, F. *Science* **1992**, *258*, 1474.

(2) (a) Kraabel, B.; McBranch, D.; Sariciftci, N. S.; Moses, D.; Heeger, A. J. *Phys. Rev. B* **1994**, *50*, 18543. (b) Kraabel, B.; Hummelen, J. C.; Vacar, D.; Moses, D.; Sariciftci, N. S.; Heeger, A. J.; Wudl, F. *Phys. Rev. B* **1994**, *50*, 18543. (c) Moses, D.; Dogariu, A.; Heeger, A. J. *Chem. Phys. Lett.* **2000**, *316*, 356.

(3) Brabec, C. J.; Zerza, G.; Sariciftci, N. S.; Cerullo, G.; De Silvestri, S.; Luzatti, S.; Hummelen, J. C. To be published.

(4) Yang, C. Y.; Heeger, A. J. *Synth. Met.* **1996**, *104*, 4267.

(5) Sariciftci, N. S.; Heeger, A. J. *Int. J. Mod. Phys. B* **1994**, *8*, 237.

(6) Yu, G.; Gao, J.; Hummelen, J. C.; Wudl, F.; Heeger, A. J. *Science* **1995**, *270*, 1789.

(7) Brabec, C. J.; Padinger, F.; Hummelen, J. C.; Janssen, R. A. J.; Sariciftci, N. S. *Synth. Met.* **1999**, *102*, 861.

(8) Ouali, L.; Krasnikov, V. V.; Stalmach, U.; Hadziioannou, G. *Adv. Mater.* **1999**, *11*, 1515.

(9) For reviews, see: (a) Hirsch, A. *The Chemistry of the Fullerenes*; Thieme: Stuttgart, 1994. (b) Prato, M. *J. Mater. Chem.* **1997**, *7*, 1097. (c) *Fullerenes and Related Structures*, *Topics in Current Chemistry*; Hirsch, A., Ed.; Springer-Verlag: Berlin/Heidelberg, 1999.

(10) For reviews, see: (a) Imahori, H.; Sakata, Y. *Adv. Mater.* **1997**, *9*, 537. (b) Martin, N.; Sánchez, L.; Illescas, B.; Pérez, I. *Chem. Rev.* **1998**, *98*, 2527. (c) Imahori, H.; Sakata, Y. *Eur. J. Org. Chem.* **1999**, 2445.

(11) Liu, S.-G.; Shu, L.; Rivera, J.; Liu, H.; Raimundo, J.-M.; Roncali, J.; Gorgues, A.; Echegoyen, L. *J. Org. Chem.* **1999**, *64*, 4884.

(12) Knorr, S.; Grupp, A.; Mehring, M.; Grube, G.; Effenberger, F. *J. Chem. Phys.* **1999**, *110*, 3502.

(13) Yamashiro, T.; Aso, Y.; Otsubo, T.; Tang, H.; Harima, Y.; Yamashita, K. *Chem. Lett.* **1999**, 443.

(14) Nierengarten, J.-F.; Eckert, J.-F.; Nicoud, J.-F.; Ouali, L.; Krasnikov, V. V.; Hadziioannou, G. *Chem. Commun.* **1999**, 617.

(15) van Hal, P. A.; Knol, J.; Langeveld-Voss, B. M. W.; Meskers, S. C. J.; Hummelen, J. C.; Janssen, R. A. J. *J. Phys. Chem. A* **2000**, *104*, 5974.

(16) Although OPV1-C_{60} is the smallest member of the homologous series of OPV*n*-C_{60} dyads, it lacks a vinylene bond and is therefore formally not an oligo(*p*-phenylene vinylene)-C_{60} derivative.

(17) Weller, A. *Z. Phys. Chem. Neue Folge* **1982**, *133*, 93.

(18) Stalmach, U.; Kolshorn, H.; Brehm, I.; Meier, H. *Liebigs Ann.* **1996**, 1449.

(19) Maggini, M.; Scorrano, G.; Prato, M. *J. Am. Chem. Soc.* **1993**, *115*, 9798.

(20) Although only a single vibrational progression is resolved in the spectra, several C−C stretch modes (e.g., ring and vinyl stretch modes) in the 1100−1800 cm^{-1} range are expected to contribute to the spectrum. See: Tian, B.; Zerbi, G.; Schenk, R.; Müllen, K. *J. Chem. Phys.* **1991**, *95*, 3191.

(21) Peeters, E.; Marcos, A.; Meskers, S. C. J.; Janssen, R. A. J. *J. Chem. Phys.* **2000**, *112*, 9445.

(22) Williams, R. M.; Zwier, J. M.; Verhoeven, J. W. *J. Am. Chem. Soc.* **1995**, *117*, 4093.

(23) Fluorescence spectra were corrected for the Raman scattering of ODCB or toluene by subtracting the spectrum of the pure solvents from the spectra of the OPV*n*-C_{60} solutions, after correction for the absorbed light intensity by measuring the second-order diffraction of the excitation light from the grating of the monochromator.

(24) For $n = 1$, the question of energy transfer is less relevant because the OPV1 moiety cannot be selectively excited.

(25) Dellepiane, G.; Cuniberti, C.; Comoretto, D.; Musso, G. F.; Figari, G.; Piaggi, A.; Borghesi, A. *Phys. Rev. B* **1993**, *48*, 7850.

(26) Formally, such an electron transfer could be considered as a hole transfer in which a positive charge is transferred from the fullerene to the oligo(*p*-phenylene vinylene).

(27) Although we have not studied a cosolution of OPV1 (i.e., 1,4-dimethyl-2,5-bis(2-(*S*)-methylbutoxy)benzene) with MP-C_{60}, such a mixture would not show a photoinduced intermolecular charge transfer either, because of the much higher oxidation potential of OPV1 in comparison with OPV2.

(28) Williams, R. M.; Koeberg, M.; Lawson, J. M.; An, Y. Z.; Rubin, Y.; Paddon-Row, M. N.; Verhoeven, J. W. *J. Org. Chem.* **1996**, *61*, 5055.

(29) Bell, T. D. M.; Smith, T. A.; Ghiggino, K. P.; Ranasinghe, M. G.; Shephard, M. J.; Paddon-Row, M. N. *Chem. Phys. Lett.* **1997**, *268*, 223.

(30) Llacay, J.; Veciana, J.; Vidal-Gancedo, J.; Bourlande, J. L.; González-Moreno, R.; Rovira, C. *J. Org. Chem.* **1998**, *63*, 5201.

(31) Fujitsuka, M.; Ito, O.; Imahori, H.; Yamada, K.; Yamada, H.; Sakata, Y. *Chem. Lett.* **1999**, 721.

(32) Guldi, D. M.; Maggini, M.; Scorrano, G.; Prato, M. *J. Am. Chem. Soc.* **1997**, *119*, 974.

(33) Pasimeni, L.; Maniero, A. L.; Ruzzi, M.; Prato, M.; Da Ros, T.; Barbarella, G.; Zambianchi, M. *Chem. Commun.* **1999**, 429.

(34) Brabec, C. J.; Sariciftci N. S. To be published.

(35) Roman, L. S.; Andersson, M. R.; Yohannes, T.; Inganäs, O. *Adv. Mater.* **1997**, *9*, 1164.

(36) Shaheen, S.; Brabec, C. J.; Hummelen, J. C.; Sariciftci N. S. To be published.

(37) Finder, C. J.; Newton, M. G.; Allinger, N. L. *Acta Crystallogr., Sect. B* **1974**, *30*, 411.

(38) From similar calculations for the mixture of OPV1 and MP-C_{60}, free energies for the charge-separated state of 2.87 and 1.76 eV are estimated in toluene and ODCB, respectively. Because these energies are much higher than the MP-C_{60} triplet energy, no photoinduced electron transfer is expected.

(39) (a) Marcus, R. A. *J. Chem. Phys.* **1965**, *43*, 679. (b) Marcus, R. A. *Angew. Chem., Int. Ed. Engl.* **1993**, *32*, 1111.

(40) (a) Oevering, H.; Paddon-Row, M. N.; Heppener, M.; Oliver, A. M.; Cotsaris, E.; Verhoeven, J. W.; Hush, N. S. *J. Am. Chem. Soc.* **1987**, *109*, 3258. (b) Kroon, J.; Verhoeven, J. W.; Paddon-Row, M. N.; Oliver, A. M. *Angew. Chem., Int. Ed. Engl.* **1991**, *30*, 1358.

(41) Kroon, J.; Oevering, H.; Verhoeven, J. W.; Warman, J. M.; Oliver, A. M.; Paddon-Row, M. N. *J. Phys. Chem.* **1993**, *97*, 5065.

(42) Oevering, H.; Verhoeven, J. W.; Paddon-Row, M. N.; Warman, J. M. *Tetrahedron* **1989**, *45*, 4751.